



ESA CONTRACT REPORT

Contract Report to the European Space Agency

Technical Note - Phase-II

WP2000 & WP2100

**SMOS Report on Level 3 root zone
soil moisture & DA Impact**

*Joaquín Muñoz Sabater,
Patricia de Rosnay, Clément
Albergel, Lars Isaksen*

ESA/ESRIN Contract 4000101703/10/NL/FF/fk

**European Centre for Medium-Range Weather Forecasts
Europäisches Zentrum für mittelfristige Wettervorhersage
Centre européen pour les prévisions météorologiques à moyen terme**

ECMWF

Series: ECMWF ESA Project Report Series

A full list of ECMWF Publications can be found on our web site under:

<http://www.ecmwf.int/publications/>

Contact: library@ecmwf.int

©Copyright 2014

European Centre for Medium Range Weather Forecasts
Shinfield Park, Reading, RG2 9AX, England

Literary and scientific copyrights belong to ECMWF and are reserved in all countries. This publication is not to be reprinted or translated in whole or in part without the written permission of the Director-General. Appropriate non-commercial use will normally be granted under the condition that reference is made to ECMWF.

The information within this publication is given in good faith and considered to be true, but ECMWF accepts no liability for error, omission and for loss or damage arising from its use.

Contract Report to the European Space Agency

Technical Note - Phase-II
WP2000 & WP2100
SMOS Report on Level 3 root zone soil moisture & DA
Impact

*Authors: Joaquín Muñoz Sabater,
Patricia de Rosnay,
Clément Albergel,
Lars Isaksen*

ESA/ESRIN Contract 4000101703/10/NL/FF/fk

European Centre for Medium-Range Weather Forecasts
Shinfield Park, Reading, Berkshire, UK

February 2014

| | Name | Company |
|---|------|-----------|
| First version prepared by (April 2013) | | ECMWF |
| Quality Visa | | ECMWF |
| Application Authorized by | | ESA/ESRIN |

Distribution list:

ESA/ESRIN

Susanne Mecklenburg

ESA ESRIN Documentation Desk

SERCO

Raffaele Crapolicchio

ESA/ESTEC

Matthias Drusch

ECMWF

HR

Division & Section Heads

Contents

| | | |
|----------|--|-----------|
| 1 | Introduction | 2 |
| 2 | Root-zone soil moisture algorithm and production chain | 5 |
| 2.1 | H-TESEL | 5 |
| 2.2 | CMEM | 6 |
| 2.3 | EKF | 7 |
| 2.3.1 | Product specifications | 8 |
| 2.3.2 | Observations configuration | 8 |
| 2.3.3 | SEKF setup | 9 |
| 2.3.4 | Experiments | 10 |
| 3 | Data Assimilation Impact | 11 |
| 3.1 | Soil Moisture | 11 |
| 3.1.1 | Description of the in-situ networks | 11 |
| 3.1.2 | Validation results | 14 |
| 3.2 | Soil and 2 metre temperature | 15 |
| 3.3 | Atmospheric impact | 17 |
| 3.3.1 | Precipitation | 17 |
| 3.3.2 | Mean change in the forecast field | 17 |
| 3.3.3 | Verification | 19 |
| 4 | Discussion | 32 |
| 5 | Conclusions | 33 |
| 6 | Appendix | 35 |
| 6.1 | Score cards for Autumn 2010 (September, October and November) | 35 |
| 6.2 | Normalized RMS forecast error for vector wind speed (VW) and geopotential (Z) | 37 |
| 6.3 | Normalized RMS forecast error as a function of the atmospheric level, for VW and Z | 39 |
| 7 | References | 41 |

1 Introduction

The European Space Agency (ESA) Soil Moisture and Ocean Salinity (SMOS) mission was successfully launched in November 2009. SMOS measures the surface emissivity at L-Band (1.4 GHz), providing direct information on surface soil moisture (\sim top 5 cm of the soil) over land and salinity over oceans (Kerr et al. 2010). However, for most hydrological and climate applications, knowledge of root zone soil moisture (defined as the top 1 metre of soil moisture) is required, which it is not directly available from SMOS measurements. Current space sensors do not have the capabilities to sense soil moisture beyond 5 cm, frequently less than that. Data assimilation systems are, however, an already tested alternative to propagate the shallow information contained in the remote sensed signal to deeper layers.

The main objective of the SMOS level 3 root-zone soil moisture product, described in this report, is to provide root-zone soil moisture analysis which benefit from the assimilation of SMOS measurements. To achieve this objective, the root-zone soil moisture retrieval algorithm developed by the European Centre for Medium-Range Weather Forecasts (ECMWF) optimally combines SMOS level 1 Near Real Time (NRT) brightness temperatures observations with ECMWF forward modelled brightness temperatures into an Extended Kalman Filter (EKF) based data assimilation system (Drusch et al. 2009a; de Rosnay et al. 2013; Muñoz-Sabater et al. 2012; Muñoz-Sabater et al. 2013b). Simulated brightness temperatures provide information on the model soil moisture and surface parameters. The model soil moisture accuracy benefits from the global data assimilation system that leads to accurate atmospheric and precipitation estimates. Observed SMOS brightness temperatures are directly related to surface soil moisture and surface characteristics (vegetation, soil texture, soil type, etc.). In the data assimilation system the information in large parts of the globe is assimilated and propagated in time and space by the model, having the potential to modify the vertical soil moisture profile. The EKF algorithm accounts for the model and SMOS observations uncertainties, so that the analysed soil moisture, i.e., the level 3 soil moisture, in a perfect system, constitutes an optimal combination of both SMOS and the model soil moisture estimates.

The assimilation of SMOS data influence the state of the soil, which in turn affects the exchange of energy and water fluxes between the soil and the near surface atmosphere, with potential implications in the time evolution of atmospheric variables. The impact of assimilating SMOS data in the ECMWF based EKF, from which the level 3 root-zone soil moisture product is constructed, is assessed through the impact on complementary land surface and atmospheric variables. To this end, quality controlled in-situ soil moisture observations belonging to the International Soil Moisture Network (ISMN) were compared to the soil moisture analyses at analysis time. The comparison was undertaken for the summer of 2010, a period of the year when the evaporatranspiration fluxes are stronger, and therefore it is expected that the assimilation of SMOS data provides the largest impact on the atmosphere. Additionally, surface temperature and 2 m temperature observations available in USA were compared to the analyses. The impact on atmospheric variables was evaluated through computation of the forecast skill at different forecast lead times, and compared to a control experiment which did not use SMOS data assimilation.

This report presents a first version of a data assimilation system which, for the first time, is able to use direct satellite radiances to constraint soil moisture. This is an important step towards the future operational use of remote sensed data to extract useful information on soil moisture. The results presented in this report should be considered as a further step towards a well refined system which makes the best possible use of SMOS data. Every optimal system at ECMWF benefits of many years of research and fine tuning. Concerning SMOS, lot of technical work has been dedicated to make the assimilation of raw brightness temperatures in the ECMWF EKF

feasible, and to solve many of the issues arising in a complex system as is ECMWF's Integrated Forecasting System (IFS). The assimilation system is not yet optimal and it will take advantage of deeper investigations of each component of the assimilation system. Conclusions based on the surface and atmospheric impact showed in this report, should then be taken with some caution.

In this document we report on both, the SMOS level 3 root zone soil moisture product developed and generated by ECMWF, and the impact on the new state of the soil in surface and atmospheric variables. The report includes the following components:

- A description of the production algorithm and the architecture of the production chain, based on the land surface model Hydrology Tiled ECMWF Scheme for Surface Exchanges over Land (Balsamo et al. 2009, H-TESEL), the Community Microwave Emission Modelling platform (CMEM, Drusch et al. 2009b) (de Rosnay et al. 2009a; de Rosnay et al. 2009b; Muñoz-Sabater et al. 2011c), and the ECMWF EKF land surface data assimilation system (de Rosnay et al. 2013; Muñoz-Sabater et al. 2013b),
- A presentation of the product characteristics, including resolutions, time sampling, timeliness and format,
- Results of root zone soil moisture product verification and accuracy estimates based on validation results against data from in-situ soil moisture networks, following the approach proposed by (Albergel et al. 2012a),
- An assessment of the gain/degradation in the forecast skill on several key atmospheric variables.

This work has been conducted as part of the ESA/ESRIN Contract number 4000101703/10/NL/FF/fk which supports the ECMWF SMOS data assimilation study. Although the report is reasonably self-contained, it relies on the following other documents produced in the framework of the SMOS data assimilation study. They are referred in this report for further details on SMOS data implementation at ECMWF, monitoring and data assimilation developments:

- MS1TN-P1: SMOS Global Surface Emission Model, November 2009 (de Rosnay et al. 2009b), <http://www.ecmwf.int/publications/library/do/references/show?id=89525>
- MS1TN-P2: IFS Interface, November 2009 (Muñoz-Sabater et al. 2009) <http://www.ecmwf.int/publications/library/do/references/show?id=89524>
- MS2TN-P1/2/3 Operational Pre-processing chain, Collocation software development and Offline monitoring suite, December 2010 (Muñoz-Sabater et al. 2010) <http://www.ecmwf.int/publications/library/do/references/show?id=89972>
- TN-P11-WP1100 SMOS Continuous Monitoring Report - Part 1, February 2011 (Muñoz-Sabater et al. 2011b) <http://www.ecmwf.int/publications/library/do/references/show?id=90041>
- TN-P11-WP1200 SMOS Report on data thinning, August 2011 (Muñoz-Sabater et al. 2011d) <http://www.ecmwf.int/publications/library/do/references/show?id=90042>
- TN-P11-WP1300 SMOS Report on noise filtering, November 2011 (Muñoz-Sabater and de Rosnay 2011) <http://www.ecmwf.int/publications/library/do/references/show?id=90361>
- TN-P11-WP1100 SMOS Continuous Monitoring Report - Part 2, December 2011 (Muñoz-Sabater et al. 2011a) <http://www.ecmwf.int/publications/library/do/references/show?id=90375>
- FR-PI-PI: SMOS Data Assimilation Study, Phase I, Final Report, January 2013 (Muñoz-Sabater et al. 2013b)

- TN-PII-WP1100 SMOS Continuous Monitoring Report - Part 3, April 2013 ([Muñoz-Sabater et al. 2013a](#))
- TN-PII-WP2300 SMOS report on Hot-Spots, December 2013 ([Muñoz-Sabater et al. 2013c](#))
- TN-PII-WP1100 SMOS Continuous Monitoring Report - Part 4, January 2014 ([Muñoz-Sabater et al. 2014](#))
- TN-PII-WP1400: SMOS report on Bias correction, in preparation ([de Rosnay et al. 2014](#))
- ECMWF-SMOS web page for further information
<http://www.ecmwf.int/publications/library/do/references/show?id=90041>

2 Root-zone soil moisture algorithm and production chain

The ECMWF SMOS level 3 root-zone soil moisture algorithm relies on an Extended Kalman Filter (EKF) soil moisture data assimilation system, which is part of the ECMWF Integrated Forecasting System (IFS) (Drusch et al. 2009a; de Rosnay et al. 2013; Muñoz-Sabater et al. 2013b). The EKF system merges SMOS level 1 NRT brightness temperature observations with the H-TESSSEL-CMEM simulated brightness temperatures. H-TESSSEL describes the soil moisture vertical transfer as a result of land surface processes interactions with the atmosphere. For the soil heat budget, the Fourier diffusion law is used (Balsamo et al. 2009). H-TESSSEL constitutes the surface module of the IFS and it benefits from the global 4D-VAR data assimilation system used for the upper air analysis, which provides high quality atmospheric conditions for land surface model integrations. In particular, good quality precipitation is highly relevant to simulate soil moisture dynamics. CMEM is interfaced to H-TESSSEL in the IFS and used in the EKF as forward observation operator to simulate L-band brightness temperature, as seen from SMOS (Drusch et al. 2009b; de Rosnay et al. 2009a; Muñoz-Sabater et al. 2011c). CMEM has been used for NRT SMOS brightness temperatures monitoring since 2010 (Muñoz-Sabater et al. 2010; Muñoz-Sabater et al. 2011b; Muñoz-Sabater et al. 2011a; Muñoz-Sabater et al. 2013a; Muñoz-Sabater et al. 2014) and it is a key component of the SMOS data assimilation system (Muñoz-Sabater et al. 2013b). In this section we describe the different components of the data assimilation system which constitute the SMOS level 3 root-zone soil moisture product algorithm, H-TESSSEL, CMEM and the EKF, along with a description of the main characteristics and setup of the Level 3 product. The IFS cycle 38r2 is used for these investigations.

2.1 H-TESSSEL

H-TESSSEL is the ECMWF land surface model, used for operational weather forecasting (Balsamo et al. 2009). H-TESSSEL is a point-wise model that describes soil moisture vertical diffusion using the Richards equation. On each grid point the vertical soil column is discretised on four layers (thicknesses 7 cm, 21 cm, 72 cm and 1.89 m). H-TESSSEL uses the dominant soil texture class for each gridpoint. This information is collected from the FAO (Food and Agriculture Organization). Soil types are derived from the FAO/UNESCO Digital Soil Map of the World, DSMW, which exists at a resolution of 5'x5' (about 10 km). FAO DSMW provides the information on two levels of soil depth namely 0-30 cm and 30-100 cm. Since the root zone is most important for the water holding, the 30-100 cm layer is selected for H-TESSSEL. To interpolate to model target resolution, the dominant soil type is selected. This procedure has the advantage of preserving hydraulic properties when moving across various model resolutions. The climate field used by the model has an index from 1 to 7 corresponding to the soil textures as shown in Figure 1: 'coarse' (1), 'medium' (2), 'medium fine' (3), 'fine' (4), 'very fine' (5), 'organic' (6), and 'tropical organic' (7).

Each grid box in the model is divided in up to 8 vegetation tiles (bare ground, low and high vegetation without snow, exposed snow, snow under high vegetation, interception reservoir, ocean/lakes, and sea ice). In each grid box two vegetation classes (high and low) are present. Twenty vegetation types, including deserts, ice caps, inland water and ocean, have been defined from an external data base (USGS 1999). Each vegetation type is characterized by a set of fixed parameters for the minimum canopy resistance, spatial coverage, and leaf area index, a sensitivity coefficient describing the dependence of the canopy resistance on water vapour deficit, and the root distribution over the soil layers. The fraction of a grid box covered by each of the tiles depends on the type and relative area of low and high vegetation, and the presence of snow and intercepted water.

An extensive description of the H-TESSSEL land surface model is available in the IFS online documentation (IFS documentation 2012).

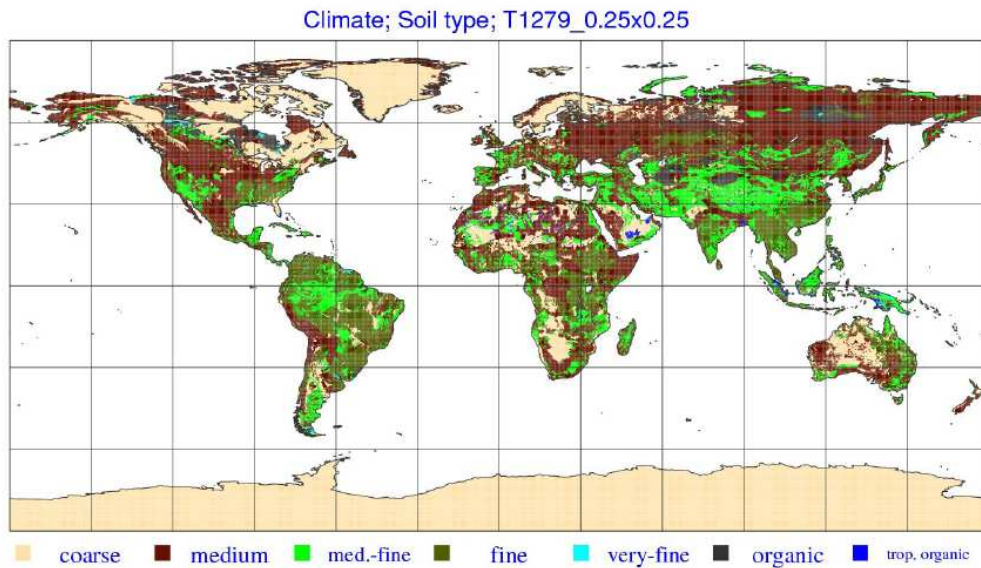


Figure 1: Soil type classes as used in H-TESSSEL (from the online IFS documentation [IFS documentation 2012](#))

2.2 CMEM

A crucial component of the SMOS brightness temperature data assimilation system is the forward model operator, which is able to bring the observations and a model equivalent of the observation to the same space for comparison purposes.

CMEM is the ECMWF forward operator for low-frequency passive microwave brightness temperatures from 1 to 20 GHz. It is a highly modular code, written in Fortran language, all this making it specially suitable for implementation within the IFS (Fig. 2). Four different modules for the soil, vegetation, snow and atmospheric microwave emission are used in CMEM. All possible combination of parameterisations implemented in CMEM are presented in <https://software.ecmwf.int/wiki/display/LDAS/CMEM+Documentation>.

In (de Rosnay et al. 2009b) a wide overview of the CMEM main physical parameterisations and other related technical documentation is provided. Relevant results compiled from three different intercomparison studies are included too, using L-band observations from the NASA Skylab mission in 1973-1974 (Drusch et al. 2009b), in situ L-band observations of the SMOSREX (Soil Monitoring Of the Soil Reservoir Experiment) site in South-West France (Muñoz-Sabater et al. 2011c), and C-band observations provided by the Advance Microwave Scanning Radiometer on Earth Observing System (AMSR-E) on the NASAs AQUA satellite over the AMMA area in West Africa (de Rosnay et al. 2009a). These studies validate the skill of CMEM to accurately represent the soil emission under different conditions. They also propose the most adequate parameterisations to be used for each component of the soil contributing to low frequencies microwave emission.

CMEM was recently introduced and interfaced to the IFS (Muñoz-Sabater et al. 2009). CMEM input data is provided by H-TESSSEL integrations, and a monthly value of LAI per type of vegetation, based on a MODIS climatology (Boussetta et al. 2013), along with other auxiliary data, is used to provide the first-guess for comparison to SMOS observations, at the time of the observations and at the model grid.

ECMWF has also developed a website with lot of information about the CMEM model. The code is freely available to the entire scientific community at the following website:

<https://software.ecmwf.int/wiki/display/LDAS/CMEM>

CMEM modules

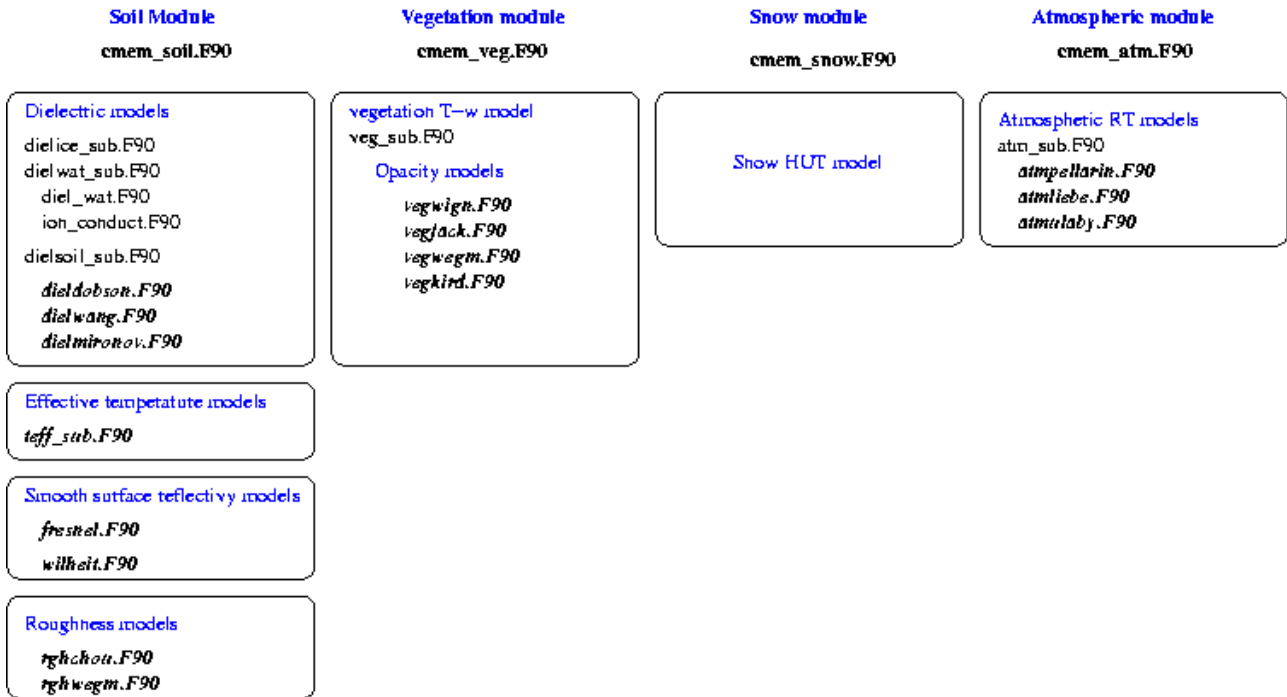


Figure 2: CMEM modular structure. For each module, the different parameterisations available are shown.

2.3 EKF

The ECMWF soil moisture analysis is based on a point-wise EKF which combines a background state and screen level variables (2 m temperature and relative humidity) and satellite observations to obtain a soil moisture product of better quality than the pure model based estimation. The analysed soil moisture state vector \mathbf{x}_a is computed at time t_i for each grid point as:

$$\mathbf{x}^a(t_i) = \mathbf{x}^b(t_i) + \mathbf{K}_i[\mathbf{y}^o(t_i) - H_i(\mathbf{x}^b)]$$

with superscripts a, b, o standing for background, analysis and observations, respectively, \mathbf{x} the model state vector, \mathbf{y} the observation vector and H the non-linear observation operator. The Kalman gain matrix \mathbf{K}_i is computed at time t_i as:

$$\mathbf{K}_i = [\mathbf{P}^{-1} + \mathbf{H}_i^T \mathbf{R}^{-1} \mathbf{H}_i]^{-1} \mathbf{H}_i^T \mathbf{R}^{-1}$$

where \mathbf{H}_i is the linearised observation operator, \mathbf{P} is the error covariance matrix associated with \mathbf{x} and \mathbf{R} is the observation errors covariance matrix. SMOS data were incorporated to this scheme, allowing observed brightness temperatures being part of the observation vector, along with the specification of its uncertainty in the \mathbf{R} covariance matrix of observation errors, and influence the soil moisture analysis (Muñoz-Sabater et al. 2013b).

In this section, the main characteristics of the Level-3 SMOS root zone soil moisture product, along with the configuration of the SMOS observations and the set up of the EKF used are specified.

2.3.1 Product specifications

The spatial resolution of SMOS observations ranges from 35 to 50 km (43 km on average over the field of view), depending on the incidence angle and the geographical location of the observation. Nonetheless, the NRT product, as received at ECMWF, is processed onto a fixed hexagonal grid with approximately 15 km node separation. Although this resolution is very close to match the ECMWF T1279 spectral resolution, in this configuration two observed brightness temperatures in consecutive nodes of the SMOS grid are found to be very correlated horizontally. These correlations are not desirable in a data assimilation system if they do not account for correlated observations. Consequently, the ECMWF spectral T511 reduced Gaussian grid (approximately equivalent to 40 km horizontal grid) was selected to process the root zone soil moisture product, because it matches better the original resolution of the SMOS observations. This does not mean that SMOS observations will be free from horizontal correlations, but in this case they will be small. Therefore, the soil moisture product will be produced and delivered at global scale in a T511 ECMWF reduced Gaussian grid.

The production period spans from the post-commissioning phase until the end of the satellite nominal life, i.e., from 1 May 2010 to 31 October 2012. The analysis are produced routinely daily at synoptic times; 0000, 0600, 1200 and 1800UTC, and it is available at the three first layers of the land surface model, i.e., from 0-7 cm, 7-28 cm and 28-100 cm. The L3 root zone soil moisture product will be delivered as an integrated value over the first 100 cm, but it is also flexible in the way it will be processed for delivery to ESA (integrated over the first metre of soil, separated for each layer, etc.). Concerning the format of the soil moisture product, it will be produced in grib format.

2.3.2 Observations configuration

The configuration in which the observations are assimilated in the EKF to produce the L3 root zone soil moisture product is based on previous reports findings (see links in section 1).

Prior to assimilation, SMOS observations were bias corrected by using a point-wise CDF matching, where the observations monthly mean and standard deviation were linearly rescaled to match that of the reference, which in this case was the model simulating brightness temperatures at the top of the atmosphere. The CDF matching technique was applied using data from the years 2010, 2011 and half of the year 2012. Then, a set of two monthly correction coefficients (one correcting for the mean value and another one for the standard deviation) were obtained individually for each month and used to eliminate systematic bias between observations and model equivalent. Although the CDF matching period may seem very short to obtain CDF monthly coefficients, a sliding window of [-2.5, +2.5] months around the middle value of each month was used, increasing the minimum number of observations necessary to obtain statistically significant values. This approach demonstrated to be superior than using single coefficients for the whole year (see more details in (de Rosnay et al. 2014)).

Only three incidence angles are being assimilated; 30, 40, and 50 degrees. Although there is no technical limitation preventing the assimilation of more incidence angles, the CDF monthly linear coefficients were optimized only for these three angles. Future versions of the L3 product, described in this report, may include larger number of incidence angles. Furthermore, the use of only three incidence angles assures a volume of observations per 12h cycle worth of data acceptable for the current computing capabilities and structure of the IFS. These angles are also less affected by angular noise (Muñoz-Sabater and de Rosnay 2011) and more data is available at intermediate incidence angles than at low incidence angles. The combined use of these three angles also guarantees the radiative transfer model to account and discriminate for the vegetation effect.

The margin around each incidence angle was fixed to 1 degree, i.e., observations in the bins [29-31], [39-41] and [49-51] are considered. For each node of the SMOS grid (the ISEA grid of the NRT product delivered to ECMWF) and angular bin, the observations were averaged with the objective of reducing angular noise. Then, all the observations belonging to a node, which is the closest to a grid point of the ECMWF T511 reduced Gaussian grid, were only considered.

The pure XX and YY polarisations are used and assimilated in the antenna reference frame, for which the model equivalents are rotated to be in the same reference than the observations. Only observations of highest quality should be assimilated, hence, in this product, only observations located in the alias free field of view are considered. The RFI flag contained in the BUFR product is also used to discard nodes affected by RFI. This filtering method based on flags does not guarantee to use observations free of RFI, but at least some of the most contaminant sources will be filtered out. Finally, it is worth mentioning that the observations are extracted from the NRT product of the reprocessed campaign, covering the whole of the years 2010 and 2011. To fill the gap until October 2012, the NRT v5.05 is used too, and this will not affect the quality of the retrievals because it is the same version in which the reprocessed product was created.

2.3.3 SEKF setup

In any assimilation system, the observations and the model equivalents are compared. The latter (for L-band brightness temperatures) is obtained through interface of CMEM with the IFS (Muñoz-Sabater et al. 2009). The parameterisations of CMEM to simulate brightness temperatures were selected as those matching best the reprocessed SMOS NRT product, in terms of minimum Root Mean Squared Difference (RMSD), minimum mean bias (MB) and best correlation (R) values (de Rosnay et al. 2014). The key CMEM parameterisations meeting these requirements were (Wang and Schmugge 1980) for the dielectric model, (Wigneron et al. 2007) for the vegetation emissivity and (Wigneron et al. 2001) for the soil roughness. The effect of the soil temperature and the atmospheric contributions in the simulated brightness temperatures were also accounted for using the parameterisations of (Wigneron et al. 2001) and (Pellarin et al. 2003), respectively. These combinations of parameterisations are also used operationally since 19 November 2013 for monitoring purposes (Muñoz-Sabater et al. 2014).

The SMOS components of the Jacobian matrix were also calibrated and made it compatible with the screen level variables. It was found that a soil moisture perturbation value between $0.005m^3m^{-3}$ and $0.01m^3m^{-3}$ was the most suited to compute the sensitivity of brightness temperatures to soil moisture perturbations. To make it compatible with the operational values used for 2 m temperature and relative humidity, this value was set up to $0.01m^3m^{-3}$. Furthermore, the maximum sensitivity allowed of model brightness temperatures to a soil moisture perturbation of $0.01m^3m^{-3}$ was set up to $250K/m^3m^{-3}$ in absolute value. Most grid points show negative jacobian values, reflecting the fact that, in general, an increased amount of water in the soil decrease the soil emissivity. Larger negative values than $250K/m^3m^{-3}$ were found in the interface between snow and snow free areas, whereas large positive values were also found in some desertic regions.

The covariance matrix of the observations errors was simplified and considered to be diagonal, with the squared pure radiometric accuracy of the observations as the variance of the diagonal elements. In this case, the correlation between different incidence angles was considered zero, whereas in reality it is expected some degree of correlation.

In this study, the full observational system for the upper air analysis, as set in operations, was used aiming at providing the best possible quality atmospheric and related land surface conditions for surface integrations.

2.3.4 Experiments

Based on the above configurations, two 2.5 years experiments were launched. The first one has as objective to produce the SMOS L3 root zone soil moisture product. It assimilates 2m temperatures and relative humidity from synoptic stations at synoptic times (00, 06, 12 and 18UTC), along with SMOS observations in 12h windows, without doing any distinction between ascending and descending orbits. Hereafter, the analysis of this experiment will be referenced as SMOS-DA.

The second experiment has exactly the same configuration than SMOS-DA. The only difference is that SMOS observations were not used in the EKF. It has the same configuration than the ECMWF operational suite but at different horizontal and vertical resolution. The latter will be, for the rest of this document our control experiment, and it is used as a reference to analyse the atmospheric impact of assimilating SMOS observations in the IFS. Hereafter, it will be named as CTRL-DA.

3 Data Assimilation Impact

The impact of assimilating SMOS data in the ECMWF EKF was evaluated by investigating the impact on land surface and atmospheric variables. A particular effort was put in estimating the impact on the soil moisture field, being this one of the two key variables measured by the SMOS platform. For the atmospheric impact, the emphasis was put in to those variables with strong link to soil moisture, i.e., air temperature and humidity at high pressure levels. In this section, firstly, a brief description of the networks used for soil moisture validation are described, followed by the soil moisture validation results and discussion. In addition, observations of soil and air temperature are used to validate the SMOS-DA analysis feedback on temperature. Radar precipitation data is also used in the USA to evaluate the precipitation forecast error, which is the main driver of soil moisture dynamics. Finally, an extensive verification of SMOS-DA in the forecast skill is presented.

3.1 Soil Moisture

It is expected that the assimilation of SMOS observations have an impact on the quality of the soil moisture field. The strategy used to check the quality of the SMOS-DA soil moisture analysis compared to CTRL-DA soil moisture analysis, is by comparing to independent in-situ soil moisture observations of several networks distributed around the world and incorporated to the International Soil Moisture Network (ISMN) database. The better spatial coverage in terms of available ground stations is found in the USA. In Fig. 3 a map of the networks available for validation activities at ECMWF is shown. In this validation exercise, in-situ data is considered as the "truth", even if in-situ observations can also be affected with significant errors, depending on the method used to measure it.

3.1.1 Description of the in-situ networks

SMOSMANIA SMOSMANIA is a long-term effort to acquire soil vertical profiles of soil moisture from 12 automated weather stations in Southwestern France. It was developed to validate remote sensing and model soil moisture estimates. SMOSMANIA is based on the existing automatic weather station network of Météo-France. The stations were selected as to form a Mediterranean-Atlantic transect following the marked climatic gradient between the two coastlines. The locations of the chosen stations are in relatively flat areas and the altitude of the highest station is 538m MSL. The three most eastward stations are representative of a Mediterranean climate. Observations from this well-monitored network have been extensively used for the validation of modeled and satellite-derived soil moisture, including ASCAT and SMOS. At each station, four soil moisture probes were horizontally installed at four depths: 5, 10, 20, and 30 cm. The ThetaProbe ML2X of Delta-T Devices was chosen because it has been used successfully during previous long-term campaigns of Météo-France and because it can easily be interfaced with automatic devices.

AMMA Three meso-scale sites were implemented in West Africa in the framework of the AMMA (African Monsoon Multidisciplinary Analysis) project, which aims at improving the understanding and modelling capabilities of the effect of land surface processes on monsoon intensity, variability and predictability. The three sites are located in Mali (4 stations), Niger (3 stations) and Benin (3 stations), providing in this way information along the north-south gradient between Sahelian and Soudanian regions. Soil moisture and other data are collected at different stations within the three meso-scale sites. The same installation protocol is used for all the soil moisture stations, where Time Domain Reflectometry sensors are used (Campbell CS616). TDR measurements are based on the relationship between the dielectric properties of soils and their moisture content. When

they were not suitable (e.g. due to soil texture), Delta-T ThetaProbes were used. Data were collected at a depth of 5 cm.

NRCS-SCAN A total of 177 stations from NRCS-SCAN network were used in this study. This network (<http://www.wcc.nrcs.usda.gov/scan/>) spans over all US, and provides comprehensive information of soil moisture and climate, designed to support natural resource assessments and conservation activities with a focus on agricultural areas in the United States. Climate modeling and agricultural studies have benefited from this network. Long data records of soil temperature, soil moisture at several depths, soil water level, air temperature, relative humidity, solar radiation, wind, precipitation, and barometric pressure, among others, are available for this network. The vegetation cover at those sites consists of either natural fallow or short grass. Concerning soil moisture, data are collected by a dielectric constant measuring device, and measurements are typically made at 5, 10, 20, 50, and 100cm. For this study, observations up to 1 m depth were used to build a weighted average proxy of root zone soil moisture, and used to evaluate the SMOS-DA soil moisture analysis.

USCRN The U.S. Climate Reference Network National from the Oceanic and Atmospheric Administration's National Climatic Data Center (USCRN NOAA's NCDC) consists of 114 stations developed, deployed, managed, and maintained by the National Oceanic and Atmospheric Administration (NOAA). This network was built with the purpose of detecting the national signal of climate change. Soil moisture probes were installed at five standard depths; 5, 10, 20, 50 and 100 cm.

Maqu The Maqu soil moisture and soil temperature monitoring network was established in July 2008 in the source region of the Yellow River to the south of Maqu County in Gansu province, China. The network, consisting of 20 stations, monitors the soil moisture and soil temperature at various depths (from 5 to 80 cm below the surface) at 15-min intervals. In this study, soil moisture observations at 5 cm were used.

SWATMEX In 2008, the SMOSMANIA network was extended Eastwards, with nine new stations, all of them located in an area of Mediterranean climate. The new stations are in a relatively flat terrain and at different altitudes, being the "Mazan-Abbaye" station that located at a maximum altitude of 1240 m. During the installation of soil moisture probes, soil samples were collected at the four depths (5, 10, 20 and 30 cm), of the soil moisture profile in order to calibrate the probe.

VAS The Valencia Anchor Station is located towards the North-West part of the Valencia region, in the Utiel-Requena Plateau, at about 80 km from the city of Valencia. The main objective is to define and characterise a large, reasonably homogeneous and flat area, mainly dedicated to vineyards, as reference for Cal/Val activities in low-resolution large-scale pixel size satellite sensors. Soil moisture is measured through Delta-T probes at different depths. In this study, the measurements at 5 cm were used.

OzNet The OzNet network (<http://www.oznet.org.au>) is composed of 38 stations, located within the Murrumbidgee experimental catchment in southern New South Wales, Australia. Climate variations in this catchment are primarily associated with elevation, varying from semiarid in the West (altitude from 50m MSL) to temperate in the East (altitude up to 2000m MSL). The highest station is located at 937m MSL. Land use in the catchment is predominantly agricultural with some forested areas in the steeper parts of the catchment. Each soil moisture site of the Murrumbidgee network measures the soil moisture at 0-5 cm with a soil dielectric sensor (Stevens Hydraprobe) or at [0-8], [0-30], [30-60], and [60-90] cm with water content reflectometers (Campbell Scientific). As the sensor response to soil moisture may vary with soil characteristics (e.g., salinity,

density, soil type, and temperature), the sensor calibration was undertaken using both laboratory and field measurements. Reflectometer measurements were compared with both field gravimetric samples and time-domain reflectometry (TDR) measurements.

REMEDIHUS REMDHUS is a Spanish network located in a central sector of the Duero basin, which benefits of a semiarid continental Mediterranean climate. In total, twenty stations from the REMEDIHUS network are available through the ISMN website. This area is mainly flat, ranging from 700 to 900m MSL, and the land use is predominantly agricultural with some patchy forest. This network provides hourly measurements of surface soil moisture. Each station was equipped with capacitance probes installed horizontally at a depth of 5 cm. It has already been used for the evaluation of both remotely sensed and modeled soil moisture estimates

UMBRIA This in-situ soil moisture network was set up in central Italy using portable TDR (Time Domain Reflectometry) sensors to observe soil moisture. The catchment is characterized by a Mediterranean climate with average annual precipitation of about 930 mm. Soil moisture data are recorded every 30 minutes

HOBE This is a network of 30 stations located within the Skjern River Catchment in Denmark, chosen to find representative locations for the individual network stations land cover. The stations were aligned along the long-term precipitation gradient, and placed to cover the HOBE agriculture (Voulund) and forest (Gludsted) field sites, as well as the more loamy area in the east of the catchment. For the stations in agriculture fields, the most frequent crop types, namely barley, grass, wheat, maize, and potatoes, were considered. At each station Decagon 5TE sensors were installed at 0-5, 20-25 and 50-55cm depth. These sensors simultaneously measure soil moisture, temperature and electrical conductivity. The data is logged at 30 minutes interval.

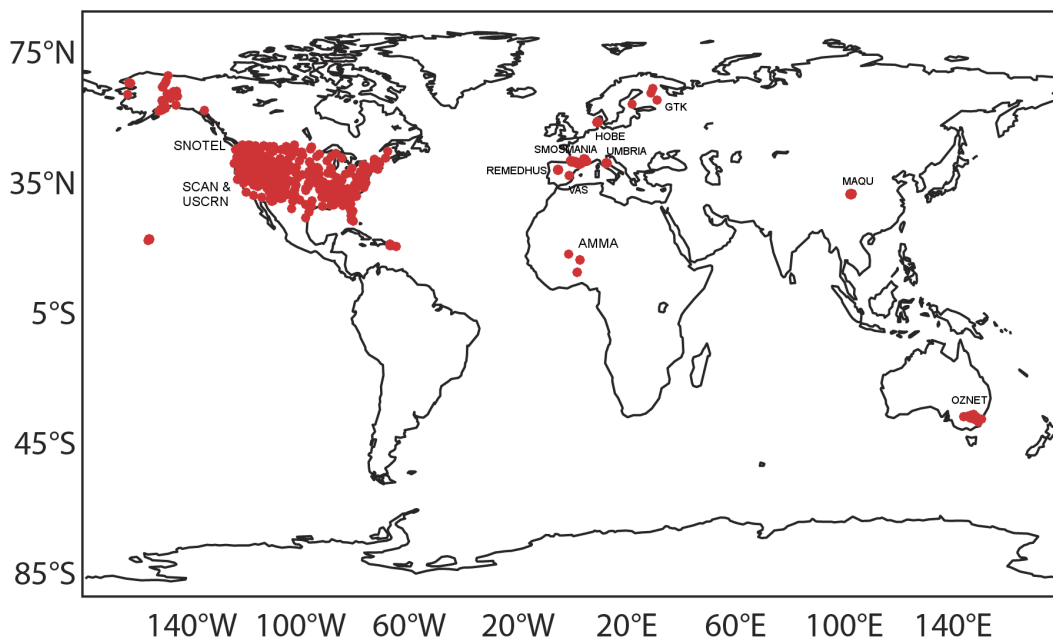


Figure 3: Soil moisture database available at ECMWF for validation activities.

3.1.2 Validation results

The period of validation in this study is the boreal summer of 2010 (June, July and August). Following the approach of (Albergel et al. 2012a), three different metrics were used: MB, RMSD and R. The p-value test (a measure of the correlation significance) was also computed, and only cases where the p-value was below 0.05 (i.e., 95% of probability that the correlation coefficient is not a coincidence) were retained. Stations with nonsignificant R values can be considered suspect and were excluded from the computation of the network average metrics.

| network | CTRL-DA | | | | SMOS-DA | | | |
|-----------|---------|-------|------|-----|---------|-------|------|-----|
| | MB | RMSD | R | N | MB | RMSD | R | N |
| SMOSMANIA | -0.017 | 0.067 | 0.77 | 9 | -0.017 | 0.063 | 0.74 | 10 |
| AMMA | -0.117 | 0.131 | 0.56 | 1 | -0.082 | 0.096 | 0.45 | 3 |
| SCAN | -0.078 | 0.132 | 0.53 | 119 | -0.072 | 0.129 | 0.53 | 119 |
| USCRN | -0.078 | 0.116 | 0.66 | 69 | -0.077 | 0.117 | 0.67 | 68 |
| MAQU | 0.027 | 0.067 | 0.75 | 16 | 0.027 | 0.067 | 0.74 | 16 |
| SWATMEX | -0.077 | 0.091 | 0.82 | 9 | -0.081 | 0.097 | 0.79 | 8 |
| VAS | -0.075 | 0.086 | 0.72 | 2 | -0.084 | 0.098 | 0.58 | 1 |
| OZNET | -0.103 | 0.121 | 0.67 | 31 | -0.103 | 0.121 | 0.70 | 31 |
| REMEDHUS | -0.065 | 0.092 | 0.57 | 17 | -0.071 | 0.094 | 0.59 | 18 |
| UMBRIA | -0.153 | 0.159 | 0.65 | 2 | -0.152 | 0.158 | 0.67 | 2 |
| HOBE | -0.052 | 0.075 | 0.70 | 29 | -0.033 | 0.067 | 0.69 | 30 |

Table 1: Mean Bias (MB), Root Mean Square Difference (RMSD) and correlation coefficient (R) values between CTRL-DA soil moisture analysis of the first seven cm of soil (using only screen-level variables) and in-situ data (in general available at, 5 cm), and between SMOS-DA soil moisture analysis (using screen-level variables and SMOS observations) and in-situ data, averaged for the period June to August 2010

Table 1 presents the MB, RMSD and R values between the CTRL-DA soil moisture analysis of the first seven cm of the soil (using only screen-level variables) and in-situ data (left panel), and between SMOS-DA soil moisture analysis (using screen-level variables and SMOS observations) and in-situ data (right panel), averaged for the period June to August 2010. The validation was carried out in a daily basis, i.e, each day the mean in-situ soil moisture value per station was computed (generally available at hourly frequency) and compared to the daily mean analysis value (available at synoptic times). The number of stations with statistically significant values for all the period of study (according to the p-value test) is also included in Table 1. Although MB and RMSD are in general quite similar, the R of the CTRL-DA analysis with in-situ data is, in average, slightly better for CTRL-DA than for SMOS-DA (R=0.67 for CTRL-DA against R=0.65 for SMOS-DA). However, these numbers have to be taken with caution, as the comparison, as displayed, is not fair. The reason is that the stations used in each network to compute statistics are not the same, and this has a strong effect over the averaged statistics. Thus, for example, for the SMOSMANIA network, the station stamped as "MTM" penalizes strongly the mean correlation of SMOS-DA, because the mean R over the three months is 0.35 and is not used for CTRL-DA. The same occurred for the SCAN network, where the "Vermillion" (R=0.30), "Mandam" (R=0.27) and "Silverswork (R=-0.57)" stations were not used in CTRL-DA, as they were not statistically significant. For the SWATMEX network, the station "MJC" obtains for CTRL-DA a R value of 0.99 with only 5 observations. And the same is valid for other networks. Consequently, to obtain a fair comparison, the databases were harmonized to use only the same stations with significant correlations for both data assimilation experiments. The harmonized results are shown in Table 2. This table clearly shows the benefits of assimilating SMOS data for the update of the soil moisture field. The R value for 8 out of the 11 networks used in this study were improved with SMOS-DA. Only SWATMEX and MAQU showed slightly worse correlation values. SWATMEX stations are located in a zone with strong slope. Many SMOS data in this area are rejected through bias correction or first-guess

check, and the impact is rather indirect. Thus, this result is not surprising. In average over the 11 networks of this study, with 284 stations with statistically significant values, the R (MB and RMSD) of SMOS-DA is improved from 0.65 ($0.078 \text{ m}^3\text{m}^{-3}$ and $0.106 \text{ m}^3\text{m}^{-3}$) for CTRL-DA to 0.68 ($0.060 \text{ m}^3\text{m}^{-3}$ and $0.101 \text{ m}^3\text{m}^{-3}$) for SMOS-DA. The analysis of SMOS-DA are chiefly overestimating the observations (except for the MAQU network), but they are closer to the observations than CTRL-DA. The largest improvements are produced in stations of REMEDHUS, OzNet, VAS and AMMA networks, all of them having the common feature of being located in semiarid climates, with long dry periods, where soil moisture retrieval from space is known to be more efficient.

In order to have an estimation of the statistical significance of these results, confidence interval estimates of the R values were computed for each network and experiment. In Fig. 4 the averaged R value (for the period June-August 2011) between analysis of SMOS-DA and in-situ data, and between CTRL-DA analysis and in-situ observations, for each network, is shown. Overlapped are the 95% confidence intervals computed by using the Fisher Z transform as in (Albergel et al. 2012a). This figure shows that, for all networks, the confidence intervals overlap for both data assimilation experiments. This means that, despite a general better representation of soil moisture by SMOS-DA, the difference of correlation is statistically non-significant. Longer evaluation periods will likely decrease the size of the confidence bars and increase the significance of these results.

| network | CTRL-DA | | | | SMOS-DA | | | |
|-----------|---------------|--------------|-------------|-----|---------------|--------------|-------------|-----|
| | MB | RMSD | R | N | MB | RMSD | R | N |
| SMOSMANIA | -0.017 | 0.067 | 0.77 | 9 | -0.015 | 0.064 | 0.78 | 9 |
| AMMA | -0.118 | 0.131 | 0.56 | 1 | -0.093 | 0.102 | 0.59 | 1 |
| SCAN | -0.079 | 0.133 | 0.54 | 115 | -0.074 | 0.130 | 0.55 | 115 |
| USCRN | -0.080 | 0.116 | 0.67 | 66 | -0.074 | 0.115 | 0.68 | 66 |
| MAQU | 0.027 | 0.067 | 0.75 | 16 | 0.027 | 0.067 | 0.74 | 16 |
| SWATMEX | -0.080 | 0.095 | 0.80 | 8 | -0.081 | 0.097 | 0.79 | 8 |
| VAS | -0.082 | 0.105 | 0.47 | 1 | -0.084 | 0.098 | 0.59 | 1 |
| OZNET | -0.104 | 0.121 | 0.67 | 31 | -0.103 | 0.121 | 0.70 | 31 |
| REMEDHUS | -0.065 | 0.093 | 0.57 | 17 | -0.067 | 0.091 | 0.61 | 17 |
| UMBRIA | -0.153 | 0.159 | 0.65 | 2 | -0.152 | 0.158 | 0.67 | 2 |
| HOBE | -0.054 | 0.078 | 0.73 | 28 | -0.032 | 0.068 | 0.73 | 28 |

Table 2: As Table 1 but each network database was harmonized to compare exactly the same stations. Bold numbers indicates that the metric is better for this experiment.

As explained in section 1, for most hydrological and climate applications, the variable of interest is the root zone soil moisture, which controls processes such as the evapotranspiration. In this study, soil measurements at 5, 10, 20, 30, 50 and 100 cm over the SCAN and USCRN networks in USA were available too during the period of study. The averaged vertical value of in-situ observations was compared to the averaged soil moisture analysis of the three first soil layers of the soil (0-100 cm), weighted by its own thickness. The results are presented in Table 3. For both networks, the R values were improved when SMOS data was assimilated. This proves the ability of the assimilation approach to propagate information on deeper layers. However, it should bear in mind that this validation exercise is not trivial, as in-situ observations at only 5 different depths are considered to sample the first meter of soil.

3.2 Soil and 2 metre temperature

Soil temperature is also an important land surface variable, with close link to many geophysical processes such as the representation of surface heat and evaporation fluxes, soil water phase change or the parameterisation of the ecosystem respiration and gross primary production, which have direct impact on the carbon pools

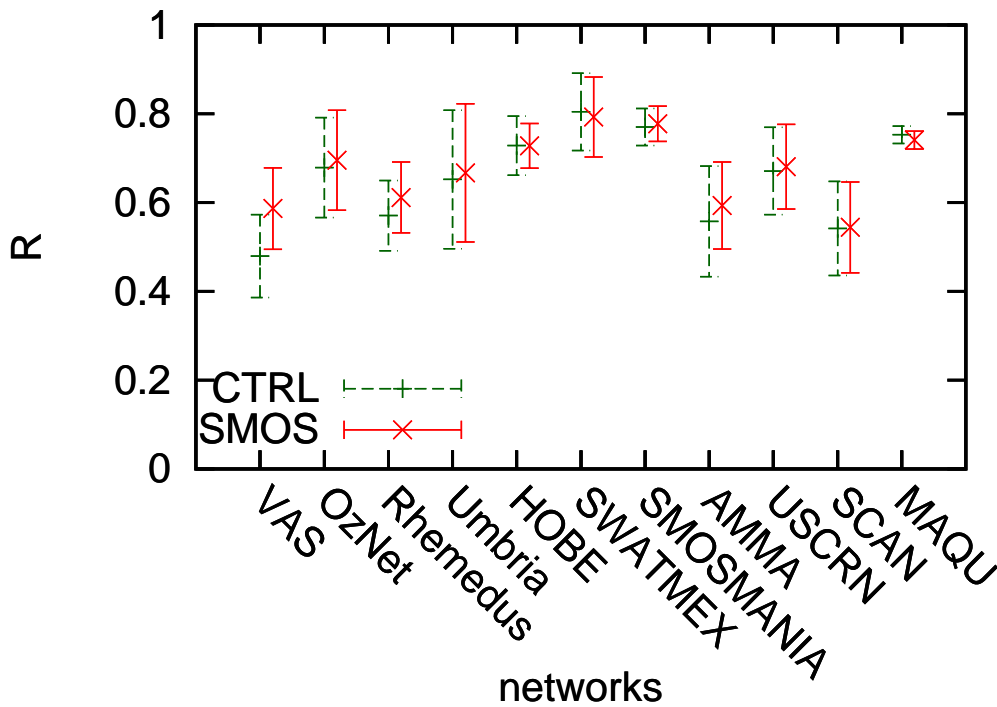


Figure 4: Averaged R value (for the period June-August 2011) between analysis of SMOS-DA and in-situ observations, and between CTRL-DA analysis and in-situ observations, for all networks used in this study. Overlapped are the 95% confidence intervals.

| network | CTRL-DA | | | | SMOS-DA | | | |
|---------|---------|-------|------|----|---------|-------|------|----|
| | MB | RMSD | R | N | MB | RMSD | R | N |
| SCAN | -0.044 | 0.113 | 0.71 | 80 | -0.044 | 0.116 | 0.72 | 80 |
| USCRN | -0.022 | 0.097 | 0.69 | 54 | -0.023 | 0.097 | 0.72 | 54 |

Table 3: Mean Bias (MB), Root Mean Square Difference (RMSD) and correlation coefficient (R) values between CTRL-DA soil moisture analysis averaged over the three first soil layers of soil (0-100 cm) and averaged in-situ data over the first metre of soil (left panel). Right panel shows the same for SMOS-DA soil moisture analysis.

estimation. The ECMWF CMEM Platform, simulating L-band brightness temperatures, uses also as input file the profile of soil temperature. Although SMOS observations reflect primarily the signal of soil moisture and vegetation state, it also contains information about soil temperature. Updating the state of soil moisture also feedbacks the soil temperature state; Hourly soil temperature observations for the summer months of 2010 are also available over the SCAN network (see 3.1.1). The ground team installed soil temperature probes at five different depths: 5, 10, 20, 50 and 100 cm. These data can be used as independent dataset for soil temperature validation. Hence, soil temperature analysis of CTRL-DA and SMOS-DA experiments were compared to soil temperature observations at 5 cm. In total 136 stations distributed from all US were used, with correlation values at 95% significant level (p-value test) for both experiments. The results showed very small impact: R= 0.803, RMSD= 4.20 K and MB= -1.01 K for CTRL-DA and in-situ data, and R= 0.804, RMSD= 4.21 K and MB=-1.05 K for SMOS-DA and in-situ data.

The same exercise that in the previous section was done for 2 m temperature, with observations belonging to the USCRN network. A weak impact was also found (not shown).

3.3 Atmospheric impact

3.3.1 Precipitation

As it was showed in (Muñoz-Sabater et al. 2013c), several zones around the world have the potential to improve the forecast of precipitation using information provided by SMOS. These zones are characterized by a strong seasonal dynamic of brightness temperatures and a good sensitivity of the model brightness temperatures to perturbations of soil moisture. Among them, the US where used in this study, as radar observations were available during the period of this study; the high-resolution NEXRAD (Next-Generation Radar) network of Doppler weather radars distributed across all US was used to verify a possible impact on precipitation. In particular, observations of precipitation data were accumulated for 6h periods. Each model forecast was initialized at 00UTC and only 24h forecasts were considered. The model prognostic precipitation was accumulated for slots of 6h, from 00 to 06UTC, 06 to 12UTC, 12 to 18UTC and 18 to 00UTC. Then the forecast error of SMOS-DA compared to CTRL-DA was computed as:

$$RMSD[PP^{OBS} - PP^{SMOS-DA}] - RMSD[PP^{OBS} - PP^{CTRL-DA}]$$

where PP accounts for the total accumulated precipitation (large scale and convective) in the forecast slot from t_1 to t_2 . Negative values means that the RMSD of CTRL-DA is greater than SMOS-DA, and in consequence an improvement by assimilating SMOS data. Positive values are a sign of precipitation forecast degradation. Fig. 5 shows the 6-hour accumulated precipitation forecast error difference between SMOS-DA and CTRL-DA, averaged for June 2010. The strongest impact is observed during the first 12 hours of forecast, in the Center of the USA, in an area where the accumulated increments of soil moisture were larger (not shown). However, there is not a clear pattern where precipitation forecast is improved or degraded. Beyond 12 h forecast, little or no impact is observed in precipitation, which suggests a very quick response of surface fluxes to the assimilation of satellite data.

3.3.2 Mean change in the forecast field

Fig 6 shows the absolute mean impact of assimilating SMOS data, on the forecast of air temperature from 2 to 5 days forecast. It is observed that up to forecast day 3, the impact is mostly concentrated into continental surfaces. This is expected because the assimilation of SMOS data is only carried out over land. After day 3, the impact starts extending to other domains, notably close to the poles. In general it can be observed a warming of the atmosphere in the USA, East of South America, North of Asia and East of Australia. On the contrary, some cooling is produced in Canada, Eurasia and some areas of Africa and South America. These patterns match well and are consistent with the mean assimilation increments (not shown). Although the values showed in this Figure are relatively low, in general, those areas where the soil is dried up due to the assimilation of SMOS data, the atmosphere is warmed up, whereas the contrary is observed when water is added to the soil. This first assessment needs however further investigation, as to understand the origin of possible systematic increments in certain areas.

Fig. 7 shows the same but for air humidity. The patterns are very similar to those of Fig. 6, but showing a clear anticorrelation with air temperature, i.e., drying of the atmosphere when the temperature is increased, and making it more humid where is cooled down.

The propagation of the mean change in the forecast into the vertical dimension is shown, for both variables, in Figs. 8 and 9, up to 5 days forecast. For air temperature, only after forecast day 4 some mean changes reach high atmospheric levels, but non of them was statistically significant. For the tropical domain (from 20 degrees

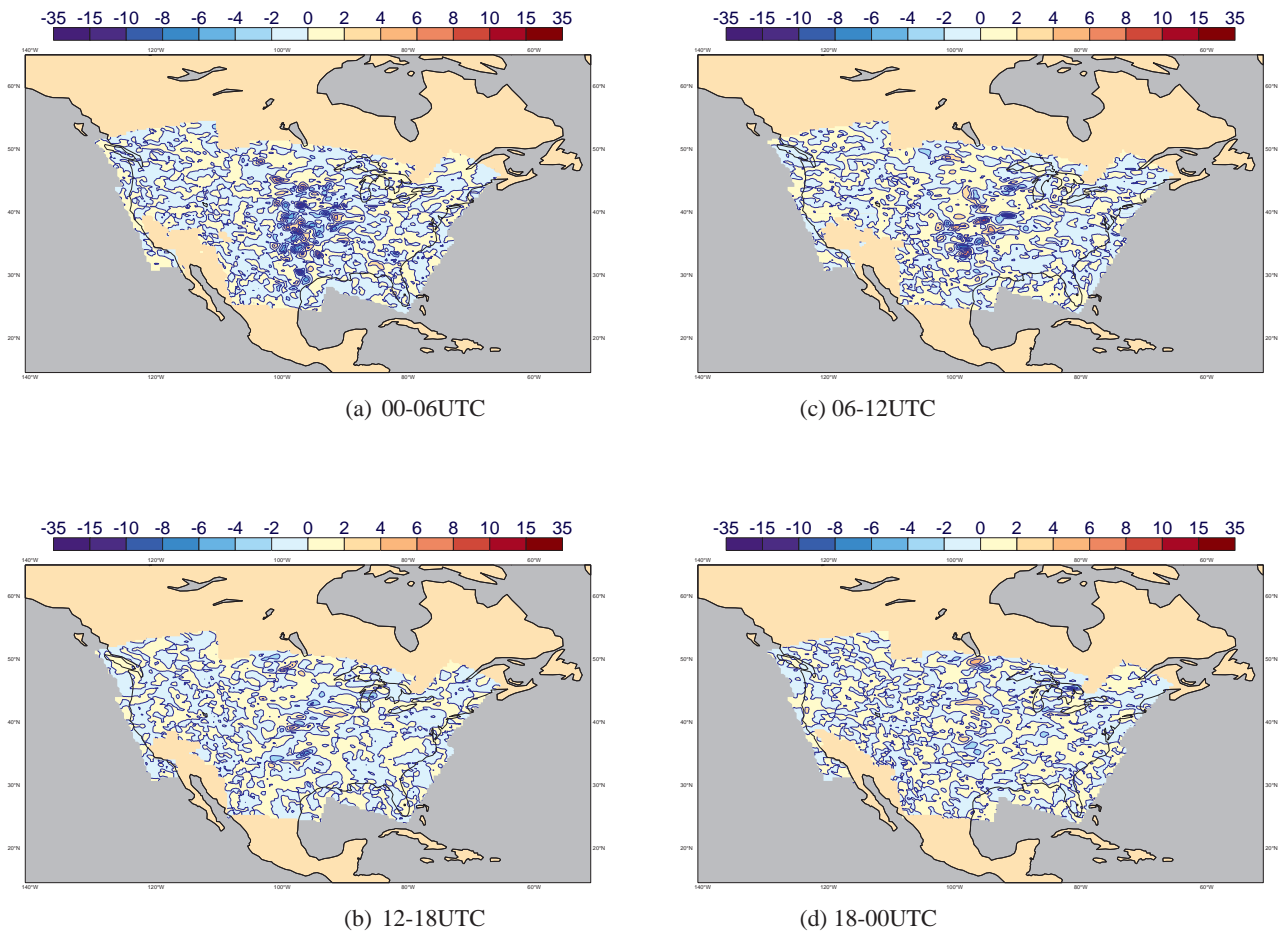


Figure 5: 6 hour accumulated precipitation forecast error difference between SMOS-DA and CTRL-DA (in mm), averaged for June 2010, for 4 different forecast times. Negative values means that the RMSD of CTRL-DA is greater than SMOS-DA, and in consequence an improvement by assimilating SMOS data. Positive values are the opposite.

South to 20 degrees North), there is not any impact. For air humidity the vertical propagation of the mean changes are rather noisy and faster, and they do not follow any marked pattern.

3.3.3 Verification

The forecast impact with soil moisture initialized from SMOS-DA compared to the initialization from CTRL-DA, in terms of objective verification scores against the own analyses, are summarised in the scorecards shown in Figs. 10 and 11. The score card provides a quick visual overview over the performance of SMOS-DA scores compared to CTRL-DA. Each symbol indicates for given time step whether or not SMOS-DA is significantly better or worse than CTRL-DA. These card shows the anomaly correlation and the root mean square (RMS) forecast error for air temperature (t) and air humidity (r) at different atmospheric levels (1000 hPa, 850 hPa, 700 hPa, 500 hPa and 200 hPa) and different domains: Northern Hemisphere, Southern Hemisphere, East of Asia, North America, Europe, Australia-New Zealand and the tropics. Table. 4 shows the geographical boundaries of these areas.

| Domain | North | West | South | East |
|-----------------------|-------|--------|-------|-------|
| Northern Hemisphere | 90.0 | -180.0 | 20.0 | 180.0 |
| Southern Hemisphere | -20.0 | -180.0 | -90.0 | 180.0 |
| East Asia | 60.0 | 102.5 | 25.0 | 150.0 |
| North America | 60.0 | -120.0 | 25.0 | -75.0 |
| Europe | 75.0 | -12.5 | 35.0 | 42.5 |
| Australia-New Zealand | -12.5 | 120.0 | -45.0 | 175.0 |
| Tropics | 20.0 | -180.0 | -20.0 | 180.0 |

Table 4: Geographical boundaries of the domains used to study the impact of SMOS-DA on the forecast skill

The forecast error for CTRL-DA ($\epsilon_{xi}^{CTRL-DA}$) and SMOS-DA ($\epsilon_{xi}^{SMOS-DA}$) experiments are defined as:

$$\epsilon_{xi}^{CTRL-DA} = fc_{xi}^{CTRL-DA} - an_{xi}^{CTRL-DA}$$

$$\epsilon_{xi}^{SMOS-DA} = fc_{xi}^{SMOS-DA} - an_{xi}^{SMOS-DA}$$

being fc_{xi} the forecast of variable x at forecast step i , and an_{xi} the own analysis of variable x at time i . In Figs. 10 and 11 the anomaly correlation difference and the RMS difference between $\epsilon_{xi}^{SMOS-DA}$ and $\epsilon_{xi}^{CTRL-DA}$ is shown. Green squares means that the anomaly correlation of SMOS-DA is better than that of CTRL-DA, or that the RMS forecast error is smaller than that of CTRL-DA, yet not significant, whereas red squares have opposite meaning. Small green triangles means that the improvement in the scores is statistically significant at 95% confidence level, whereas the big green triangles means that is statistically highly significant (the confidence bar is above zero by more than its height). Red triangles have similar meaning but they point towards degradation of SMOS-DA compared to CTRL-DA. The impact is shown up to 5 days forecast in 24 h time step, because only one daily medium-range forecast was run at 00UTC to save computing time. In total, each score averages 92 forecasts. Figs. 10 and 11 show that with the data assimilation configured as explained in sections 2.3.2 and 2.3.3, an impact of assimilating SMOS data in air temperature and air humidity forecast is obtained, mainly at the highests pressure levels, i.e., close to the surface where some impact may particularly be expected. However, the sign of the impact is very different depending on the domain under study. In general, the impact is positive in the Southern Hemisphere, whereas is negative in the Northern Hemisphere. Australia and New-Zealand, a zone very little affected by RFI, shows the best scores, whereas North America obtains the worst scores. The tropics show neutral impact. In the appendix (section 6.1), Figs. 17 and 18 show the same scores for autumn 2010. As expectec, they show much reduced impact compared to the summer period in the

Northern Hemisphere, although the results points towards the same direction that Figs. 10 and 11.

In Figs. 12 and 13 the RMS forecast error for air temperature and air humidity, normalized by the own analysis RMS, is shown up to five days forecast, in steps of 24h, for three large domains: Southern Hemisphere extra-tropics region (left column), tropics (middle column) and Northern Hemisphere extra-tropics (right column), and for atmospheric levels of 1000 (bottom), 850 hPa (middle bottom), 500 hPa (middle top) and 200 hPa (top). The period of verification is summer 2010 (June, July and August). These plots are complementary of those shown in Figs. 10 and 11, as they show the strenght of the forecast skill improvement or degradation. Negative values in these plots mean a reduction of the RMS forecast error of SMOS-DA compared to CTRL-DA, whereas positive values show degradation. Fig. 12 shows a slight improvement of air temperature forecast in the Southern Hemisphere, although these values are mostly non significant because the error bars cross frequently the zero line. Only a significant improvement of 0.8% in air temperature is obtained at 5 days forecast range and medium atmospheric pressure levels. This figure also shows neutral impact in the tropics, whereas the forecast error is significantly increased in the Northern Hemisphere, mainly at 1000 hPa, from 0.5% to 1.4%. For air humidity (Fig. 13) most scores are not significant, as most of them cross the zero line. In the appendix (section 6.2) the same figures are presented for the vector wind speed and geopotential. These two variables are also affected by interactions with air temperature and air humidity. In the Southern Hemisphere, the vector wind speed and the geopotential are significantly improved, for the lowest atmospheric levels after forecast day 4, up to 1% and 1.3% , respectively. On the contrary, in the Northern Hemisphere, a slight degradation for the geopotential, up to 1%, can be observed.

In Fig. 14 maps of the root mean square forecast error difference between SMOS-DA and CTRL-DA are shown, for 2 m temperature. These maps complement previous figures, as they make it possible to localize those regions where the largest improvements or forecast degradations are found for air temperature in the very near surface. They are shown from 24 h to 120 h forecast, i.e., from 1 to 5 days forecast. Negative values means decrease of the error forecast using SMOS data assimilation. It is shown that in general the impact is small, frequently below 1 K, even after 5 days forecast. Some few consistent improvements can be observed in the Southern Hemisphere, although they are confined to small regions. The most clear signal is a slight increase of the air temperature forecast error in center of USA, which is consistent with previous figures. For the rest of the globe, patchy small improvements or degradations were found, many of them non statistically significant.

The atmospheric vertical profile of the normalized RMS forecast error difference, for air temperature and air humidity, as a function of the latitude, is shown in Figs. 15 and 16. They are shown from 12-hour to 5 day lead forecast time. Blue values show an improvement of SMOS-DA forecast, whereas red values present a degradation. Crosses within the plots means statistically significant improvement or degradation. The Southern Hemisphere, for air temperature, is dominated by blue colour, especially after forecast day 4. This reflects progressively improvement, however these values are statistically not significant. For the Northern Hemisphere, the general trend is degradation, with some significant values close to the surface, in the band extending from 30 to 60°N latitude. This is an area which in 2010 was heavily affected by Radio Frequency Interference. The scores for the air humidity are very little affected, showing most of the time neutral impact (Fig. 16). Figs. 21 and 22 of the appendix (section 6.3) shows the same plots, for vector wind speed and geopotential. They reflect some significant improvement in the Southern Hemisphere for both variables, from near surface level up to 400 hPa, after forecast day 4.

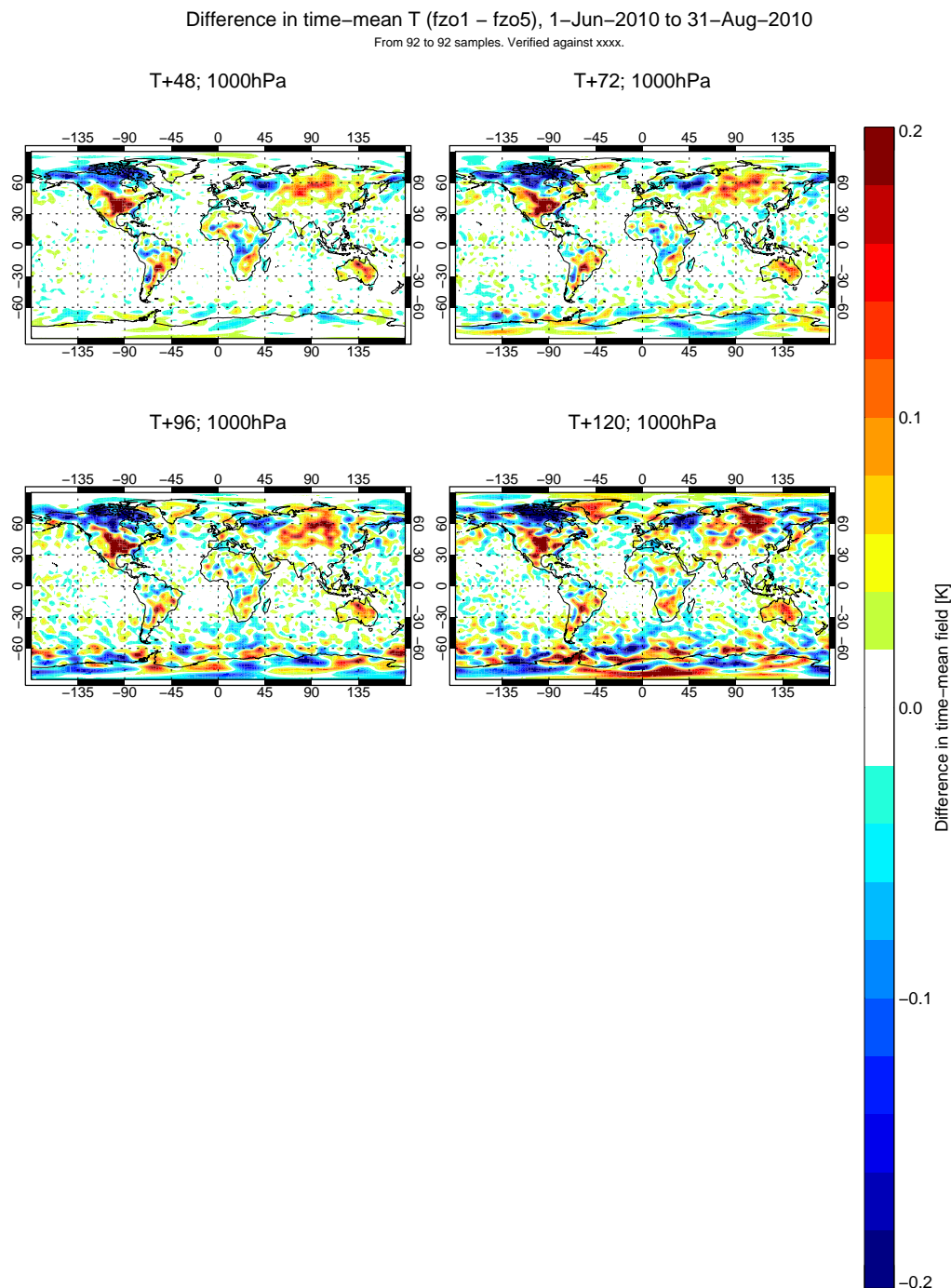


Figure 6: Absolute mean change difference in the forecast of air temperature between SMOS-DA and CTRL-DA, at 1000 hPa, averaged for the period June to August 2010. "fzo1" makes reference to SMOS-DA, whereas "fzo5" makes reference to CTRL-DA. Positive values means that SMOS-DA is warming up compared to CTRL-DA, whereas negative values points towards SMOS-DA cooling down compared to CTRL-DA.

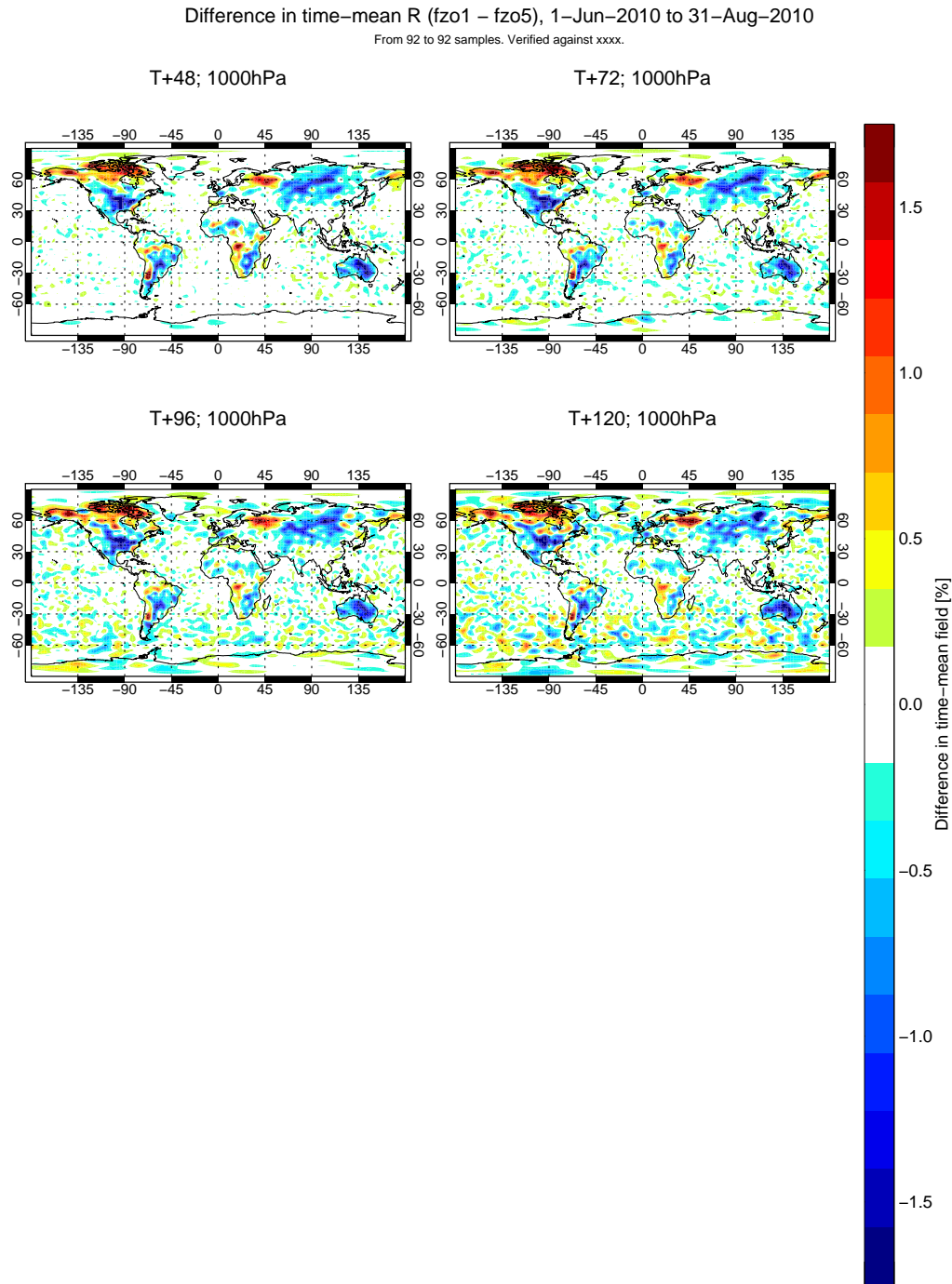


Figure 7: As Fig. 6 but for air humidity at 1000 hPa.

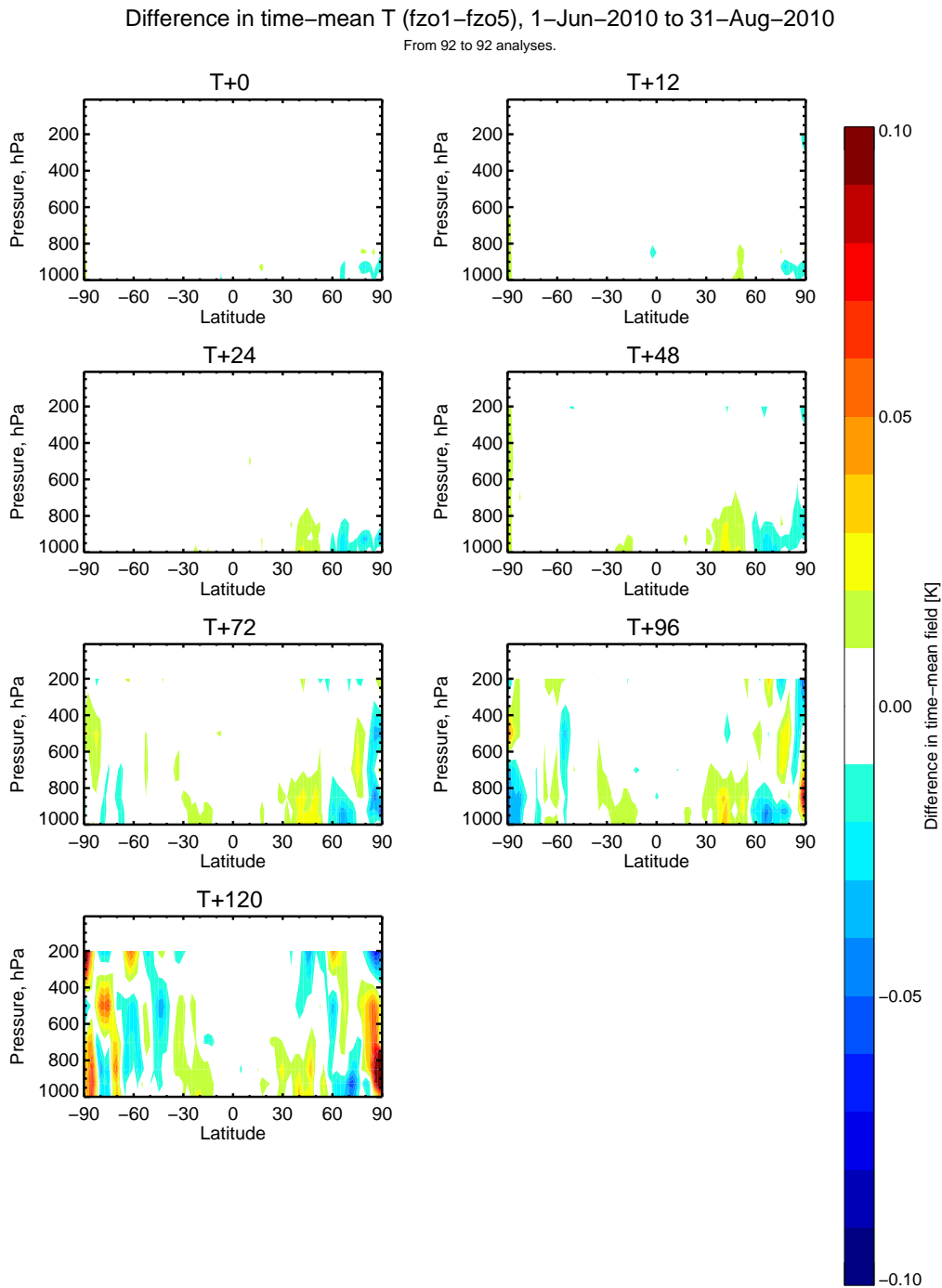


Figure 8: Absolute mean change difference in the forecast of air temperature between SMOS-DA and CTRL-DA, as a function of the atmospheric pressure level, averaged for the period June to August 2010. "fzo1" makes reference to SMOS-DA, whereas "fzo5" makes reference to CTRL-DA. Positive values means that SMOS-DA is warming up compared to CTRL-DA, whereas negative values points towards SMOS-DA cooling down compared to CTRL-DA.

Difference in time-mean R (fzo1-fzo5), 1-Jun-2010 to 31-Aug-2010

From 92 to 92 analyses.

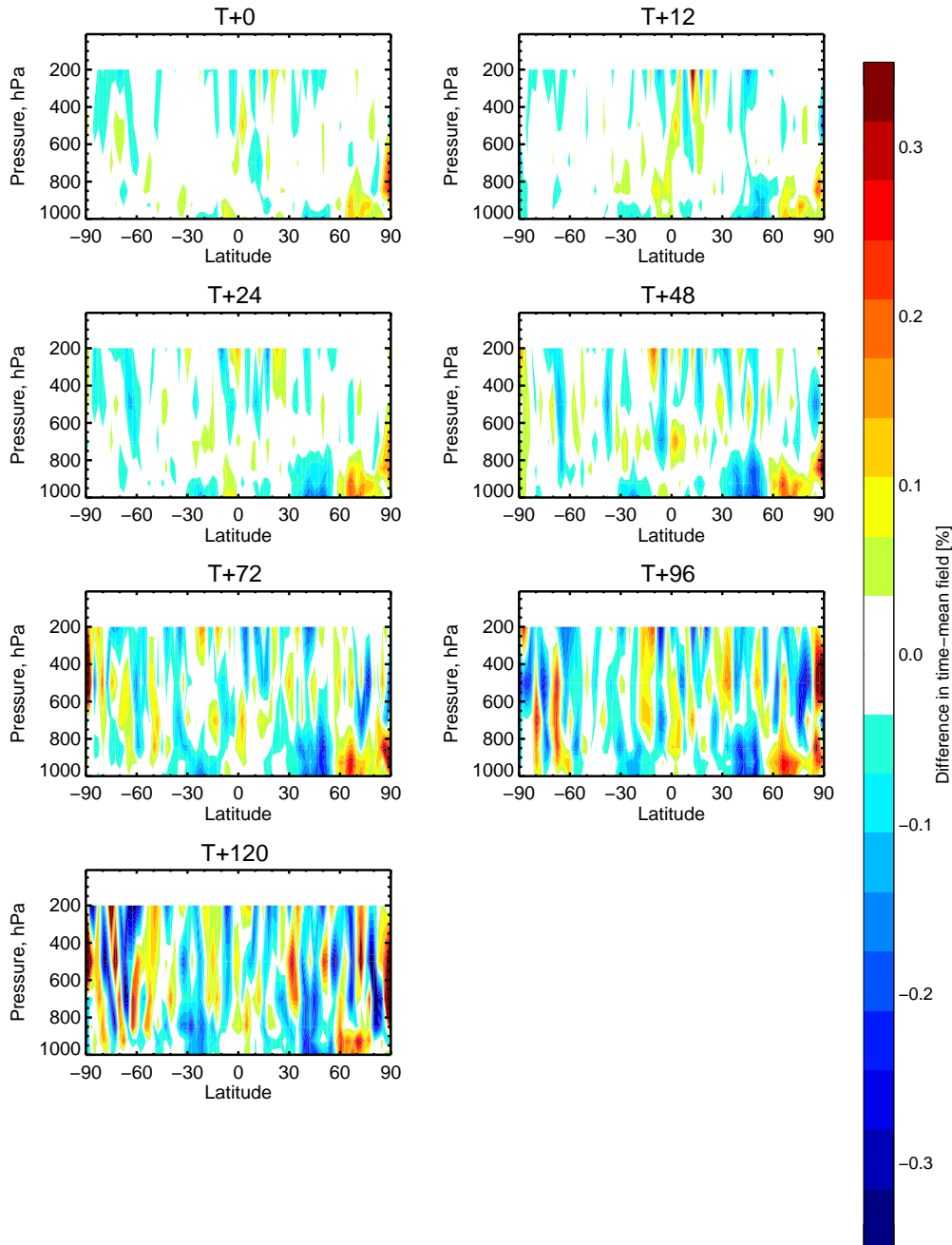


Figure 9: As Fig. 8 but for air humidity.

| | | ccaf | rmsef |
|--------|---|---------|-------|
| e.asia | r | 200hPa | ▼ |
| | | 500hPa | ▼ |
| | | 700hPa | |
| | | 850hPa | |
| | | 1000hPa | |
| | t | 200hPa | ▼ |
| | | 500hPa | |
| | | 700hPa | |
| | | 850hPa | ▼▼ |
| | | 1000hPa | ▼▼ |
| europe | r | 200hPa | ▼ |
| | | 500hPa | ▼ |
| | | 700hPa | |
| | | 850hPa | |
| | | 1000hPa | ▼ |
| | t | 200hPa | ▼ |
| | | 500hPa | ▼ |
| | | 700hPa | ▲ |
| | | 850hPa | ▼▼ |
| | | 1000hPa | ▼▼ |
| n.amer | r | 200hPa | ▼ |
| | | 500hPa | |
| | | 700hPa | |
| | | 850hPa | ▼▼ |
| | | 1000hPa | ▼▼ |
| | t | 200hPa | ▼ |
| | | 500hPa | |
| | | 700hPa | ▼▼ |
| | | 850hPa | ▼▼ |
| | | 1000hPa | ▼▼ |
| n.hem | r | 200hPa | |
| | | 500hPa | |
| | | 700hPa | |
| | | 850hPa | |
| | | 1000hPa | ▼ |
| | t | 200hPa | ▼ |
| | | 500hPa | |
| | | 700hPa | |
| | | 850hPa | ▼▼ |
| | | 1000hPa | ▼▼ |

Figure 10: Score card providing an overview over the performance of the SMOS-DA scores compared to CTRL-DA. Each symbol indicates for a given time step whether or not the experiment is significantly better or worse than the control; Green squares means that SMOS-DA is better than CTRL-DA, yet not significant. Red squares have opposite meaning. Small green triangles means that the improvement in the scores of SMOS-DA is statistically significant at 95% confidence level, whereas big green triangles means that is statistically highly significant (the confidence bar is above zero by more than its height). Red triangles have similar meaning but they point towards degradation of SMOS-DA compared to CTRL-DA. No colour means neutral impact.

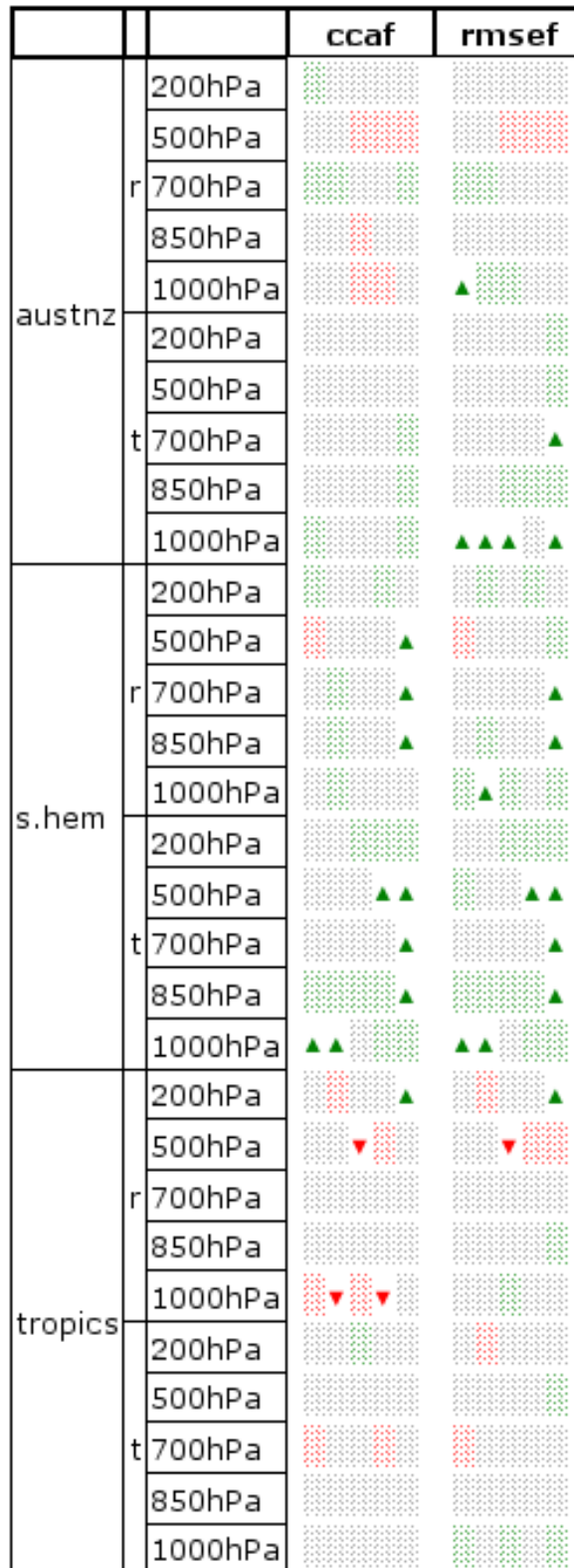
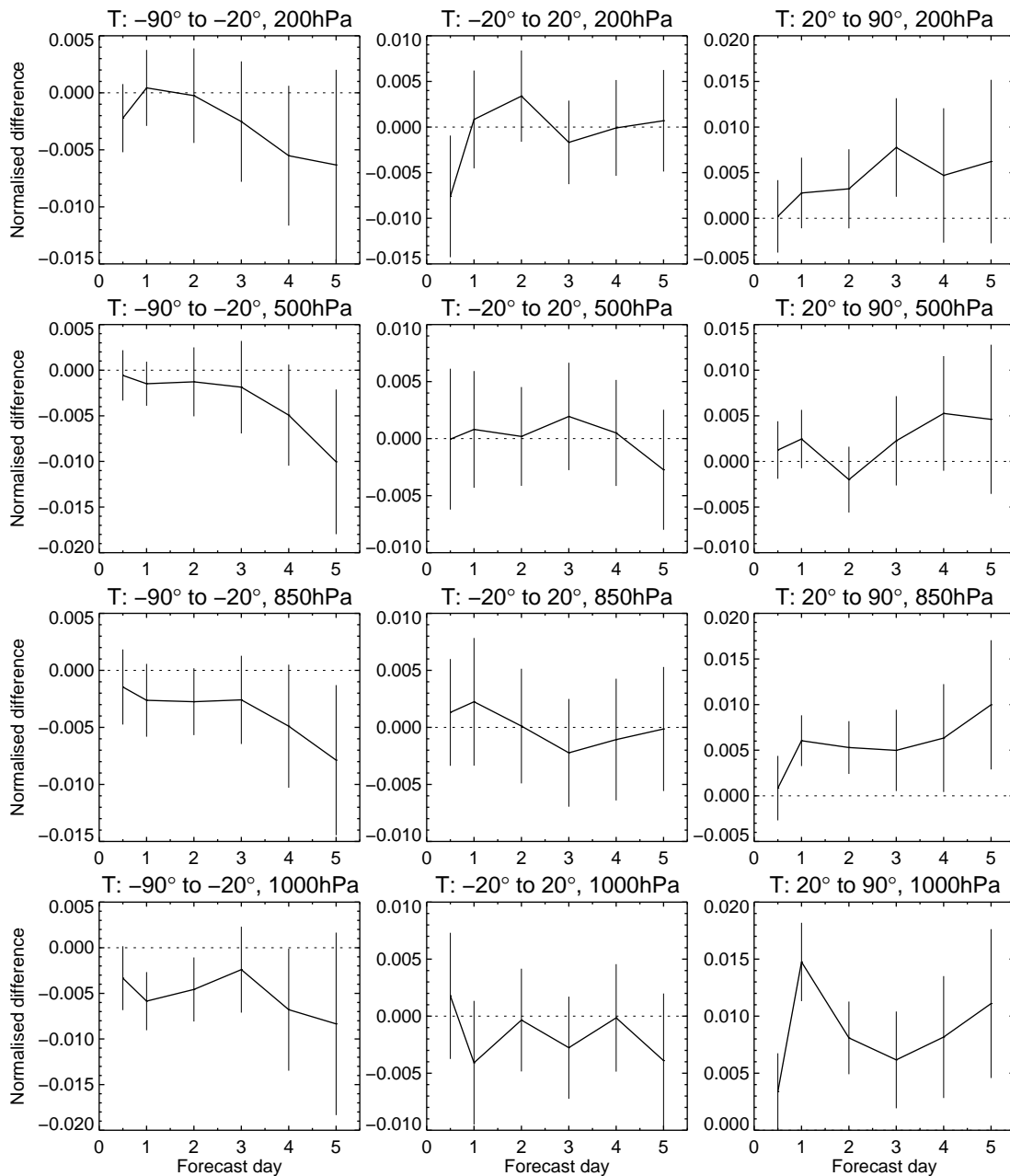


Figure 11: As Fig. 10 but for tropics and Southern Hemisphere domains.

1-Jun-2010 to 30-Aug-2010 from 87 to 91 samples. Confidence range 95%. Verified against own-analysis.



fzo1 - fzo5

Figure 12: Normalized root mean square air temperature forecast error difference between SMOS-DA and CTRL-DA, averaged for the period June to August 2010. Forecast errors are computed against the own experiment analyses. Vertical bars show 95% confidence intervals. Left column is for the Southern Hemisphere extra tropical region, middle column for tropics and right column for Northern Hemisphere extra tropical region. Top row is for 200 hPa, middle top is for 500 hPa, middle bottom is for 850 hPa and bottom row is for 1000 hPa.

1-Jun-2010 to 30-Aug-2010 from 87 to 91 samples. Confidence range 95%. Verified against own-analysis.

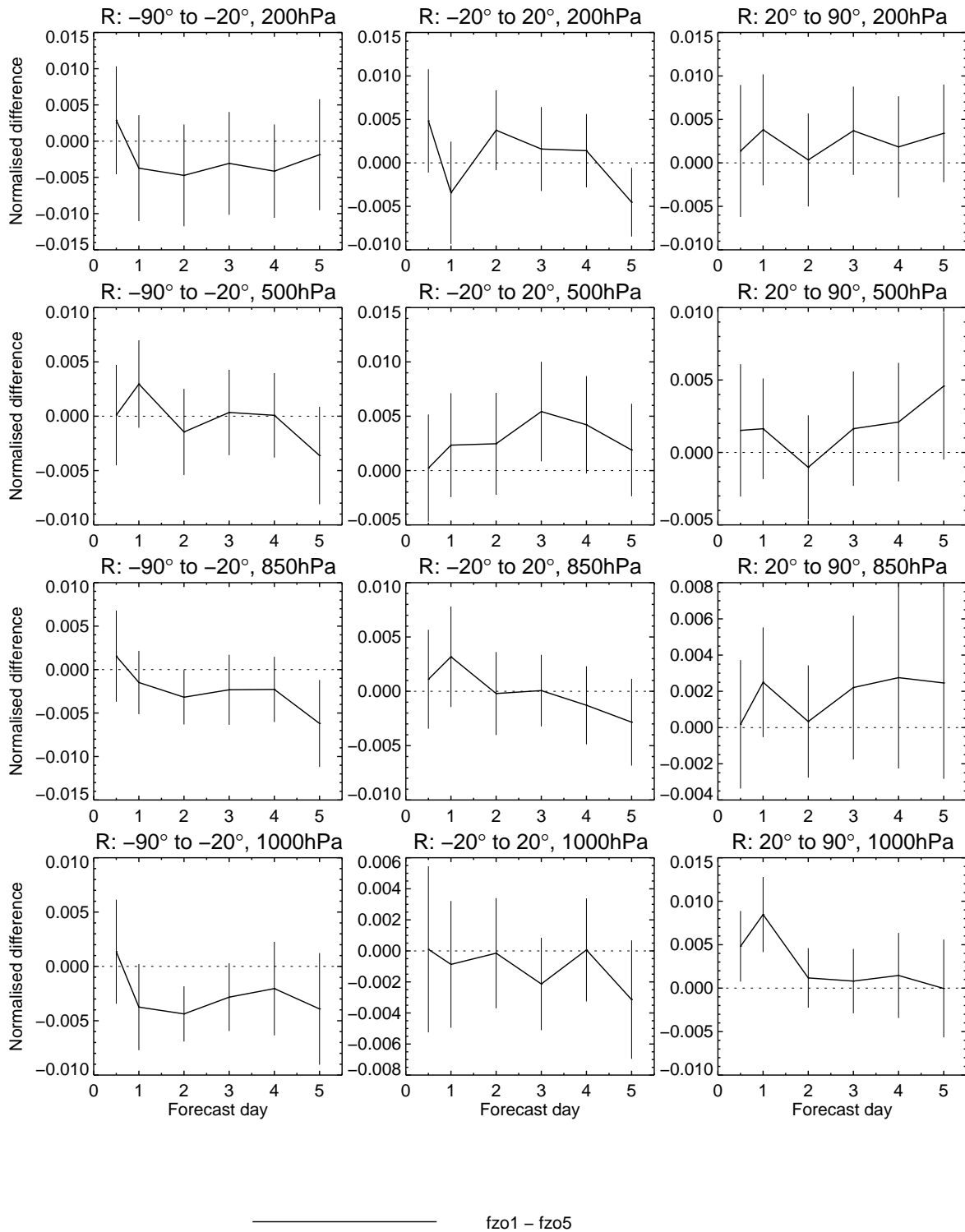


Figure 13: As Fig. 12 but for air humidity.

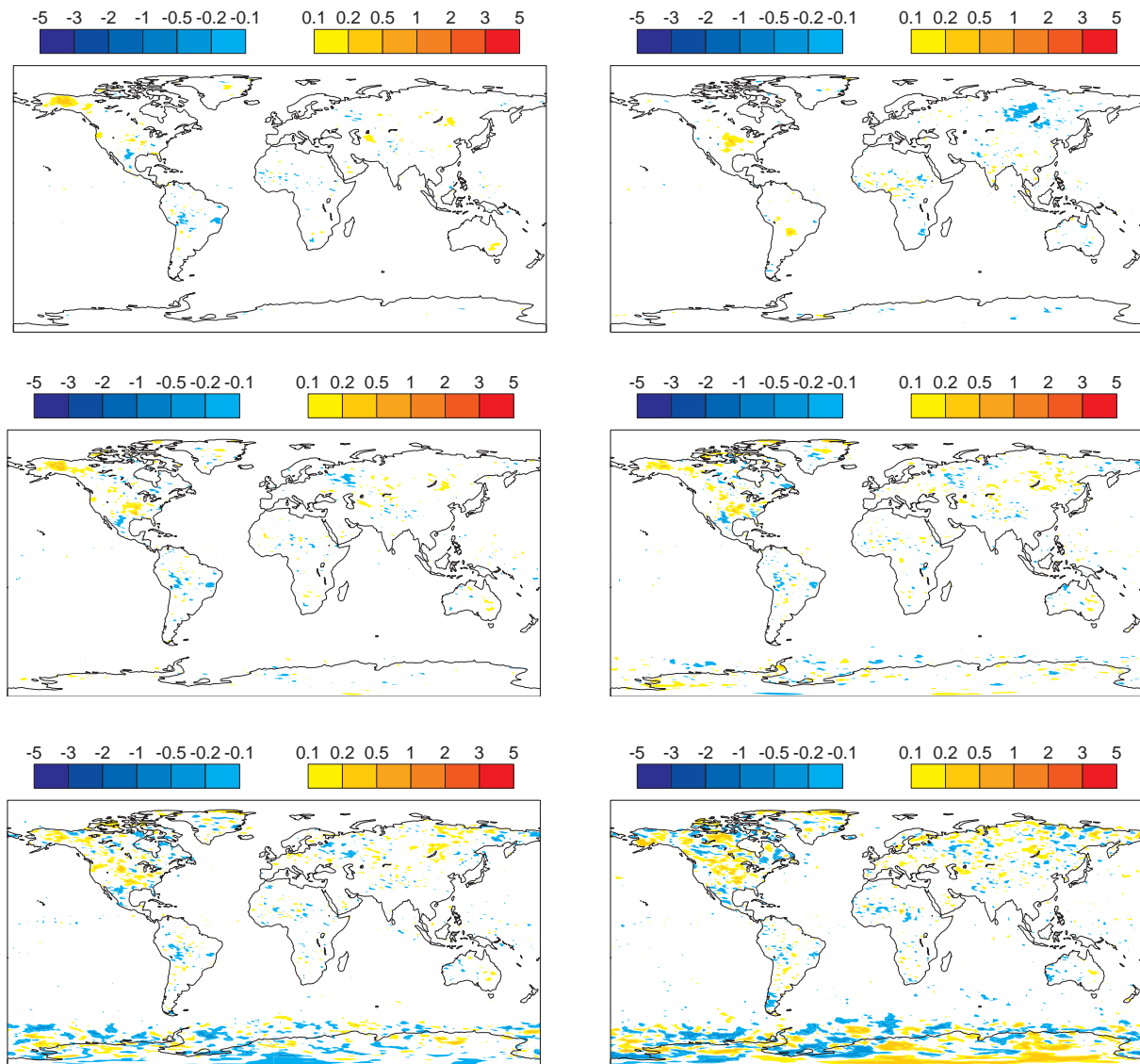


Figure 14: Root Mean Square 2 m temperature forecast error difference between SMOS-DA and CTRL-DA at 24h (top left), 36h (top right), 48h (middle left), 72h (middle right), 96h (bottom left) and 120 (bottom right) forecast lead time. Forecast errors are computed against the own experiment analysis. Values are averaged over the period June to August 2010.

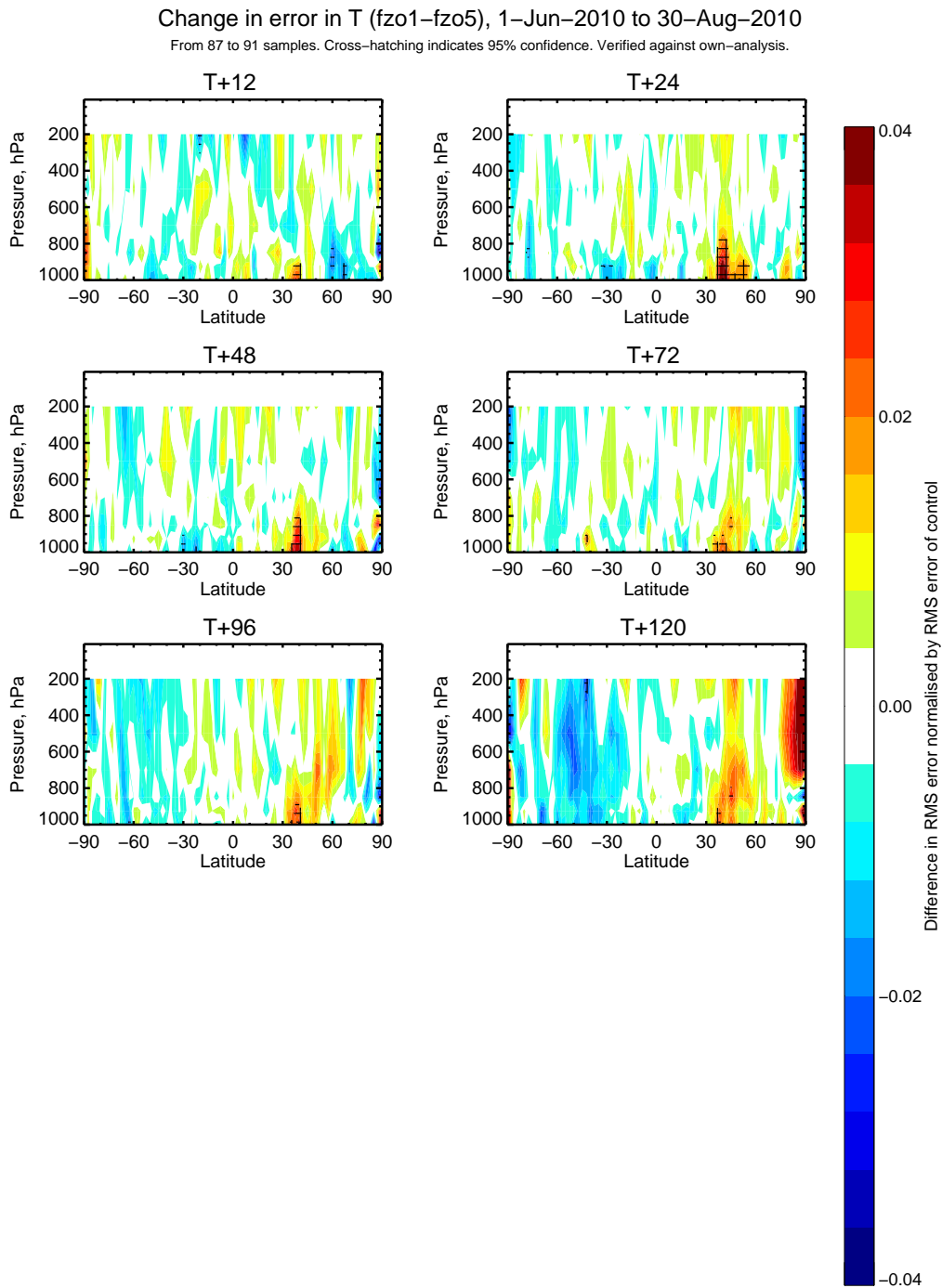


Figure 15: Normalized Root Mean Square (RMS) air temperature forecast error difference between SMOS-DA and CTRL-DA, as a function of the pressure level. Forecast errors are computed against the own experiment analyses. Values are averaged between June and August 2010. Negative values means that the RMS forecast error is smaller for SMOS-DA, whereas positive values means increase of RMS forecast error. Hatched values are significant at 95% confidence level.

Change in error in R (fzo1-fzo5), 1-Jun-2010 to 30-Aug-2010

From 87 to 91 samples. Cross-hatching indicates 95% confidence. Verified against own-analysis.

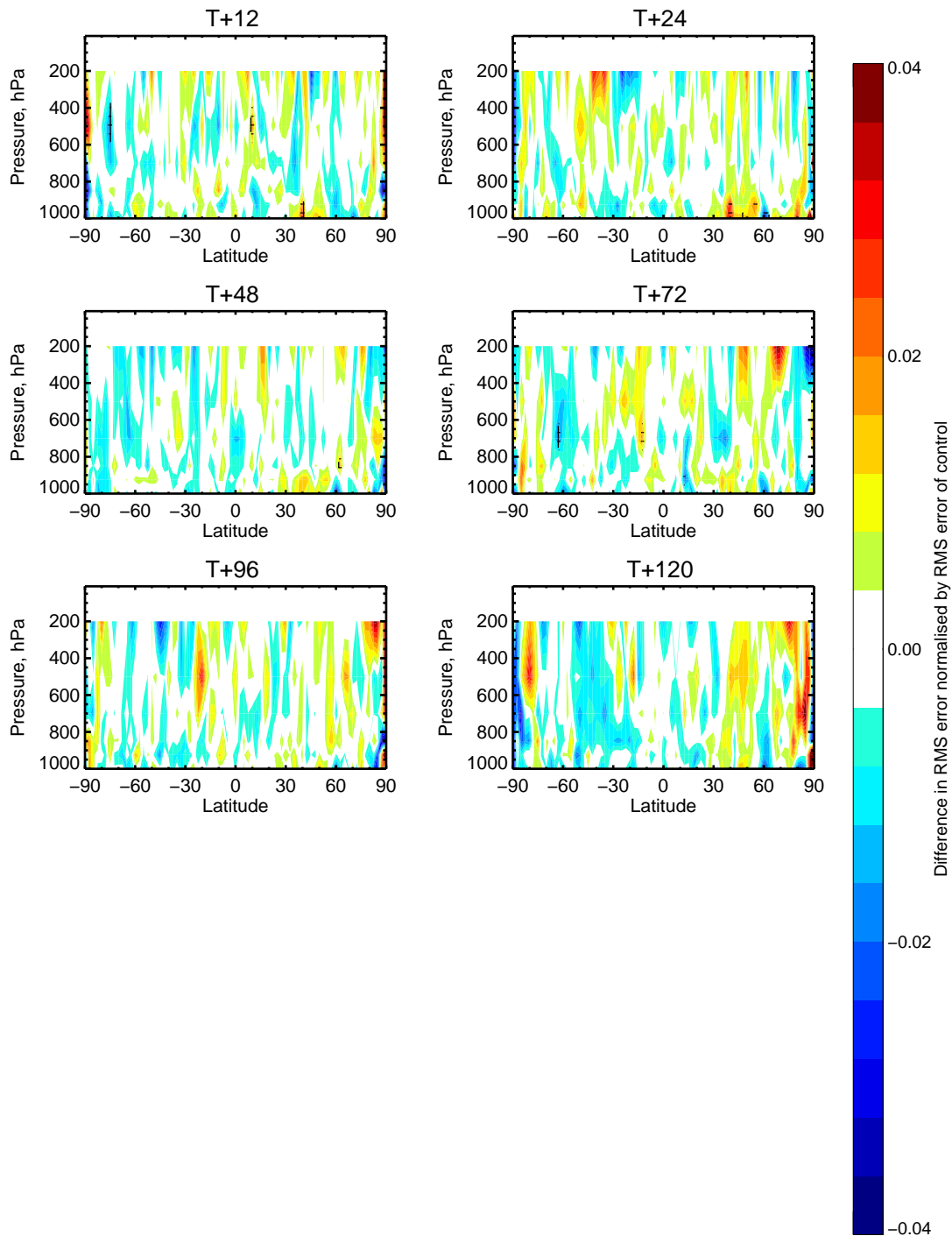


Figure 16: As Fig. 15 but for air humidity.

4 Discussion

This report describes the system that is used to generate a new root zone soil moisture product, based on the assimilation of screen level variables and SMOS data. The new product will be delivered as a 2.5 years product, covering the nominal life of the SMOS mission. SMOS data is only sensitive to soil moisture variations of the first few cms of soil, however, advanced data assimilation systems, as the EKF used in this study, makes it possible to propagate SMOS information into deeper layers through the Jacobian matrix and data assimilation cycling. In this way, not only the most shallow surface benefits from remote sensing data, but also the root-zone layer.

This is the first time that a long assimilation experiment using SMOS data has been run at ECMWF. It is also the first time that satellite radiances, at global scale, are integrated in the surface analysis. The quality of the product described in this study depends on the ability to separate the observations of only highest quality, but it is also very sensitive to the configuration of the assimilation system. The latter involves an accurate knowledge of the uncertainty assigned to the observations and the state vector, as well as knowledge of the acceptable quality control limits of the difference between the observed SMOS brightness temperature and its model equivalent simulated by CMEM. The EKF configuration used in this study benefits from previous investigations which optimize several components of the EKF, as the SMOS components of the Jacobian matrix and a dedicated monthly CDF matching removing systematic bias and variability between SMOS observations and model equivalents. It also makes better use of SMOS observations, for example, by averaging observations in angular bins of 2 degrees prior to be assimilated. However, the system is not fully optimized yet. Further refinement and deeper investigation of each of the EKF components affecting the analysis will very likely lead to improved results. Therefore, the quality of the soil moisture product presented here, as well as the atmospheric impact on several atmospheric variables presented in the above figures, should be interpreted with some caution, as they are obtained with a first version of the data assimilation system. Future investigations will target to make better use of SMOS data in the EKF, through a better quality control and through optimization of each component of the assimilation system.

The atmospheric impact shown in this study presents some positive and significant results for the Southern Hemisphere, whereas some are negative in the Northern Hemisphere. In particular, some statistically significant degradation was found close to the surface in the latitudinal band extending from 30 to 60°N North. This is the band of latitude most affected by RFI, and it might partly explain the bad scores presented in some of the figures. However, this problem cannot fully explain the negative scores obtained in some domains, in particular in the USA. Here, model aspects or non optimized components of the assimilation system might affect negatively the influence of the new state of the soil on the forecast of atmospheric variables. It should also be taken into account, that the period of verification uses SMOS observations of the reprocessed dataset. While the reprocessed dataset in 2010 removes much of the strongest RFI sources encountered during this early stage of the SMOS mission, it does certainly not remove all of it, and significant contamination could be found in the data.

Finally, it is important to understand how the atmospheric scores are verified. In this study, an analysis valid at the same time of the forecast is considered to represent the "truth", and we use each experiment's "own analysis" as the reference to compare against. In this way we avoid making a prior assumption about which analysis (SMOS-DA or CTRL-DA) is best. However, this way of verifying atmospheric scores has to be taken with caution, as they are in no way independent of the system being tested (Geer et al. 2010) and may change the level of variability which unfairly can be interpreted as negative impact. While, in this study, this choice does not seem to affect the computed scores, it does certainly need to be accounted for in the interpretation of

the results.

5 Conclusions

This document reports on 1) the system used to produce a new root zone soil moisture product assimilating screen level variables and SMOS data and 2) the impact of SMOS-DA on surface and atmospheric variables. The system benefits from the coupled HTESSEL-IFS and the CMEM interface structure, which makes it possible to compare SMOS observations and the model equivalents at the time of the observations. Previous works (see references section 1), permitted to solve some issues and make the use of SMOS data in the IFS more optimal.

An extensive validation of the impact of assimilating SMOS data in the ECMWF EKF on soil moisture, was done. To this end, independent in-situ soil moisture observations from several networks around the world were used. The period of validation was June, July and August of the year 2010. During this period, a stronger impact of the new state of the soil on atmospheric variables may be expected in the Northern Hemisphere. The soil moisture validation exercise showed that, over the eleven networks with available soil moisture observations used in this study, eight obtained better averaged R values when SMOS data was assimilated than without them. Besides, the three networks where R was not improved present particular difficult conditions, as being in areas of extreme climate of strongly contaminated by RFI. Consistently, RMSD and MB were also decreased in the experiment using SMOS data, but RMSD values remains in many cases high. This might be a consequence of representativeness issues (for example using a different soil texture in the analysis than the in-situ station), topography, vegetation, pedotransfer functions, which reflects the time integration of the meteorological forcing or the hydrological state of the soil, as well as the analysis. They are in agreement with previous validation studies conducted at ECMWF. It also emphasizes the fact that the true information content in modelled soil moisture not necessarily relies in their absolute magnitudes but in their time variation (Albergel et al. 2012b). The general trend of the soil moisture analysis increments during summer 2010 was drying the soil up. This may be an indication of the usefulness of SMOS information, as previous studies found systematic errors in the ECMWF land surface model, resulting in too wet soil conditions. However, further investigation is needed to understand a possible systematic sign of the increments in certain areas, as after bias correction, the assimilation increments are deemed to correct only for random errors and not the systematic biases.

In this study, some observations up to 100 cm deep were available over the USA too. The averaged in-situ observations were compared to the averaged soil moisture analysis over the first metre of soil, and either for the SCAN or USCRN networks, the R was improved too. The impact on soil temperature and 2 m temperature did not show significant differences.

The impact of SMOS-DA on the forecast skill of several atmospheric variables was evaluated too. It was found that the mean change in air temperature and humidity fields was mostly limited to the near surface atmosphere over continental surfaces. This result was expected as the assimilation of SMOS data is made only over land. A warming of the near surface atmospheric level was observed in areas where, in general, the soil was dried up. Similarly, a cooling of the lowest atmospheric levels was produced if moisture was added to the soil. Nonetheless, the absolute mean changes values remained low. For air humidity, the opposite sign was found, as air temperature and air humidity are anticorrelated. These results showed a clear link of the soil moisture state with air temperature and air humidity. Indeed, this has been the reason for many years (given the lack of reliable remote sensing data sensitive to soil moisture) to operationally assimilate 2 m temperature and relative humidity to constrain soil moisture. It was also found that the propagation of the mean changes in air temperature were slow in higher atmospheric levels, with almost no changes in the tropics domain. Tropical regions are dominated by high dense vegetated canopies, where SMOS has very little impact.

Although the scores here presented suggested a decrease of the forecast error for air temperature and air humidity in the Southern Hemisphere, and an increase in the Northern Hemisphere, most of these scores were shown not to be statistically significant. Just in a few cases an improvement/degradation of up to 1% was found for air temperature, but also for the vector wind speed and the geopotential. These latter variables are also affected for changes in temperature and humidity. It may be necessary to run longer experiments to ensure statistically significant results.

This report showed that ECMWF has developed a functioning data assimilation system able to produce a new soil moisture product, that is based on assimilating SMOS data. It showed interesting and preliminary results, with a clear impact of SMOS data on land surface and near surface atmospheric variables. However, deeper investigations are needed, which will permit to optimize the use of these data in the IFS, in synergy with other conventional and remote sensing data.

Acknowledgements

This work is funded under the ESA-ESRIN contract number 4000101703/10/NL/FF/fk. We would to thank Matthias Drusch and Susanne Mecklenburg (both ESA staff) for their involvement in this project. Also thanks to P. Lopez (ECMWF staff) for preparing the radar observations.

6 Appendix

6.1 Score cards for Autumn 2010 (September, October and November)

| | | ccaf | rmsef |
|--------|---------|------|-------|
| e.asia | r | | |
| | 200hPa | ▲ | |
| | 500hPa | ▲ | ▼ |
| | 700hPa | | |
| | 850hPa | | |
| | 1000hPa | | ▼ |
| | t | | |
| | 200hPa | | |
| | 500hPa | | |
| | 1000hPa | | ▼ |
| europe | r | | |
| | 200hPa | | |
| | 500hPa | | |
| | 700hPa | | |
| | 850hPa | | |
| | 1000hPa | ▼ | ▼ |
| | t | | |
| | 200hPa | ▼ | ▼ |
| | 500hPa | | |
| | 1000hPa | ▼ | ▼ |
| n.amer | r | | |
| | 200hPa | | ▲ |
| | 500hPa | | |
| | 700hPa | | |
| | 850hPa | ▲ | ▲ |
| | 1000hPa | | ▼ |
| | t | | |
| | 200hPa | | |
| | 500hPa | | |
| | 1000hPa | | ▼ |
| n.hem | r | | |
| | 200hPa | | |
| | 500hPa | | |
| | 700hPa | | |
| | 850hPa | | |
| | 1000hPa | | ▼ |
| | t | | |
| | 200hPa | | |
| | 500hPa | | |
| | 1000hPa | ▼ | |

Figure 17: As Fig. 10 but for the period 1 September to 30 November 2010.

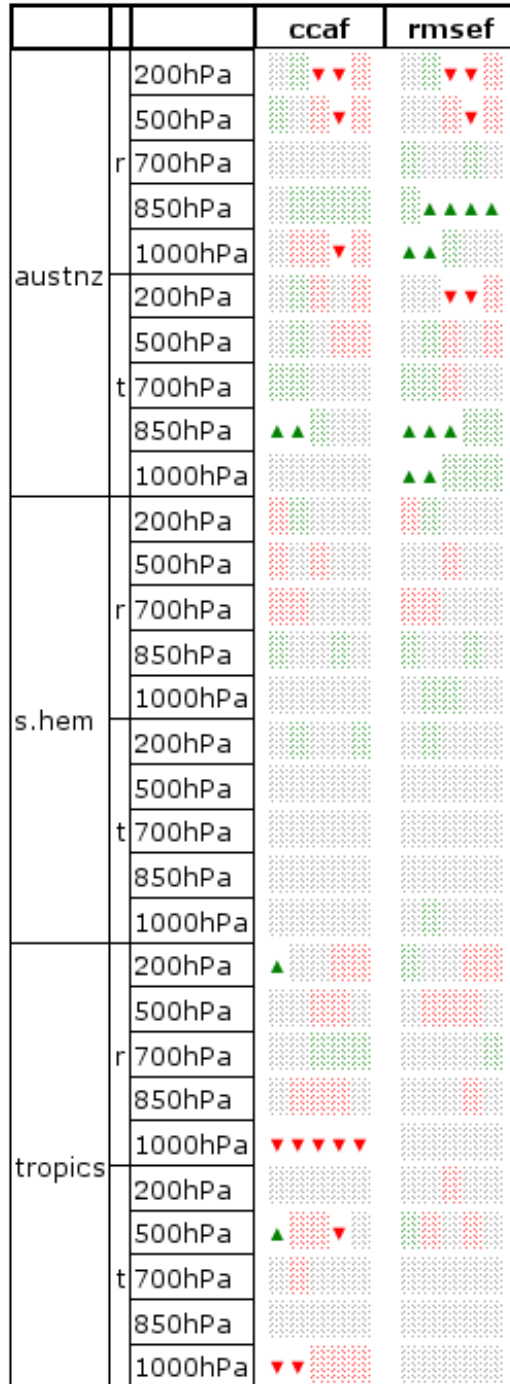
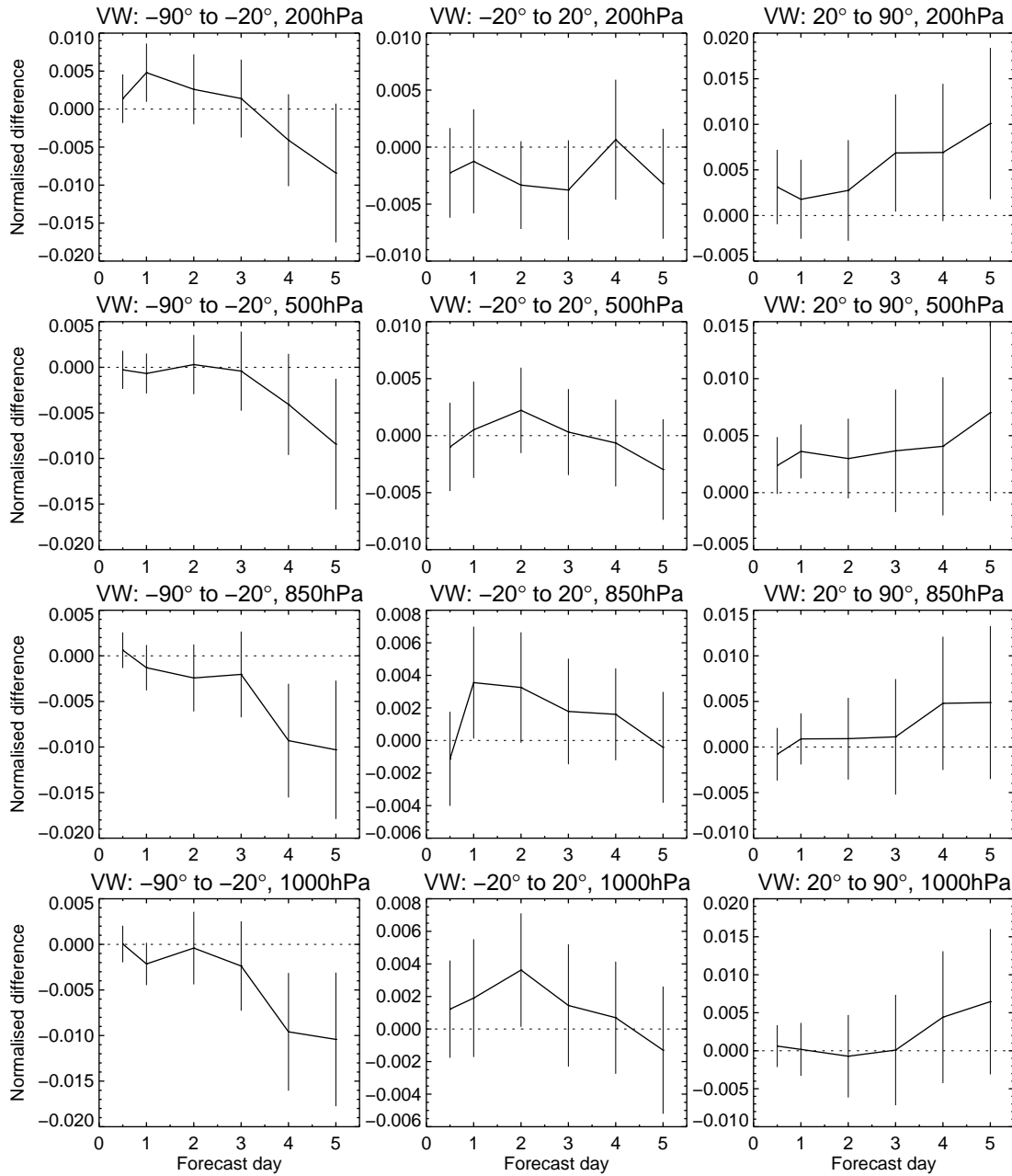


Figure 18: As Fig. 17 but the tropics and Southern Hemisphere domains.

6.2 Normalized RMS forecast error for vector wind speed (VW) and geopotential (Z).

1-Jun-2010 to 30-Aug-2010 from 87 to 91 samples. Confidence range 95%. Verified against own-analysis.



fzo1 - fzo5

Figure 19: As Fig. 12 but for the vector wind speed.

1-Jun-2010 to 30-Aug-2010 from 87 to 91 samples. Confidence range 95%. Verified against own-analysis.

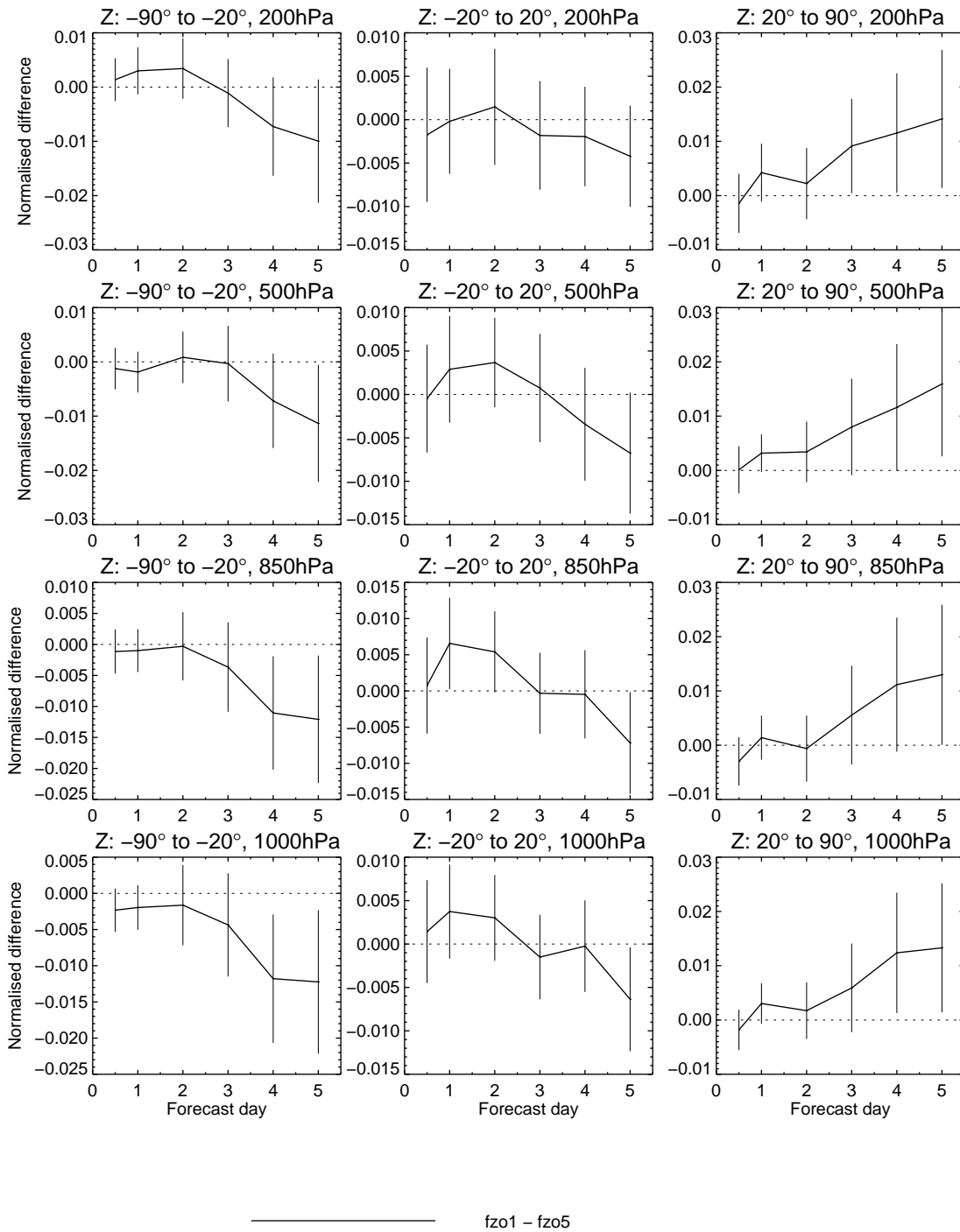


Figure 20: As Fig. 12 but for geopotential.

6.3 Normalized RMS forecast error as a function of the atmospheric level, for VW and Z.

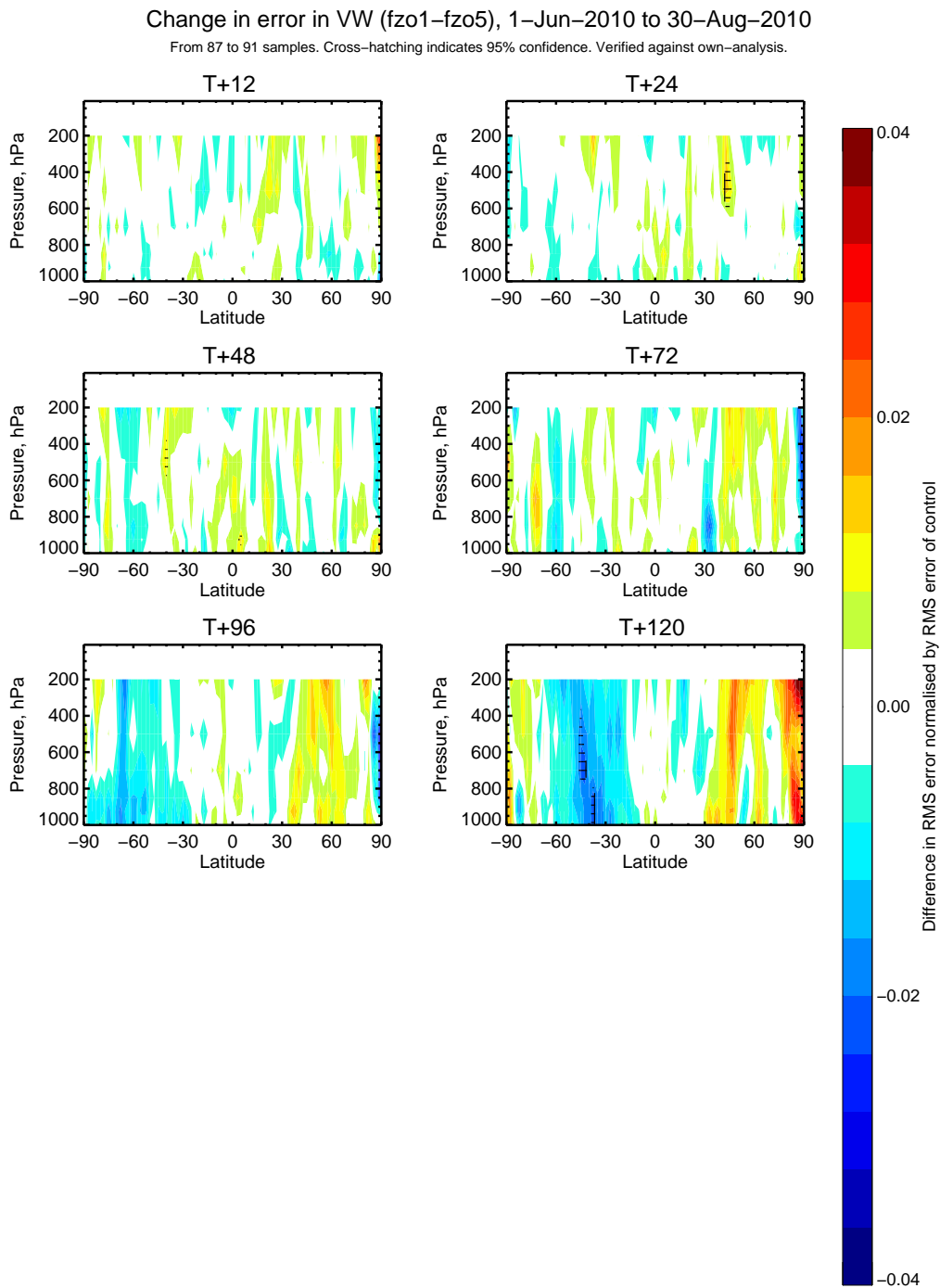


Figure 21: As Fig. 15 but for the vector wind speed.

Change in error in Z (fzo1-fzo5), 1-Jun-2010 to 30-Aug-2010

From 87 to 91 samples. Cross-hatching indicates 95% confidence. Verified against own-analysis.

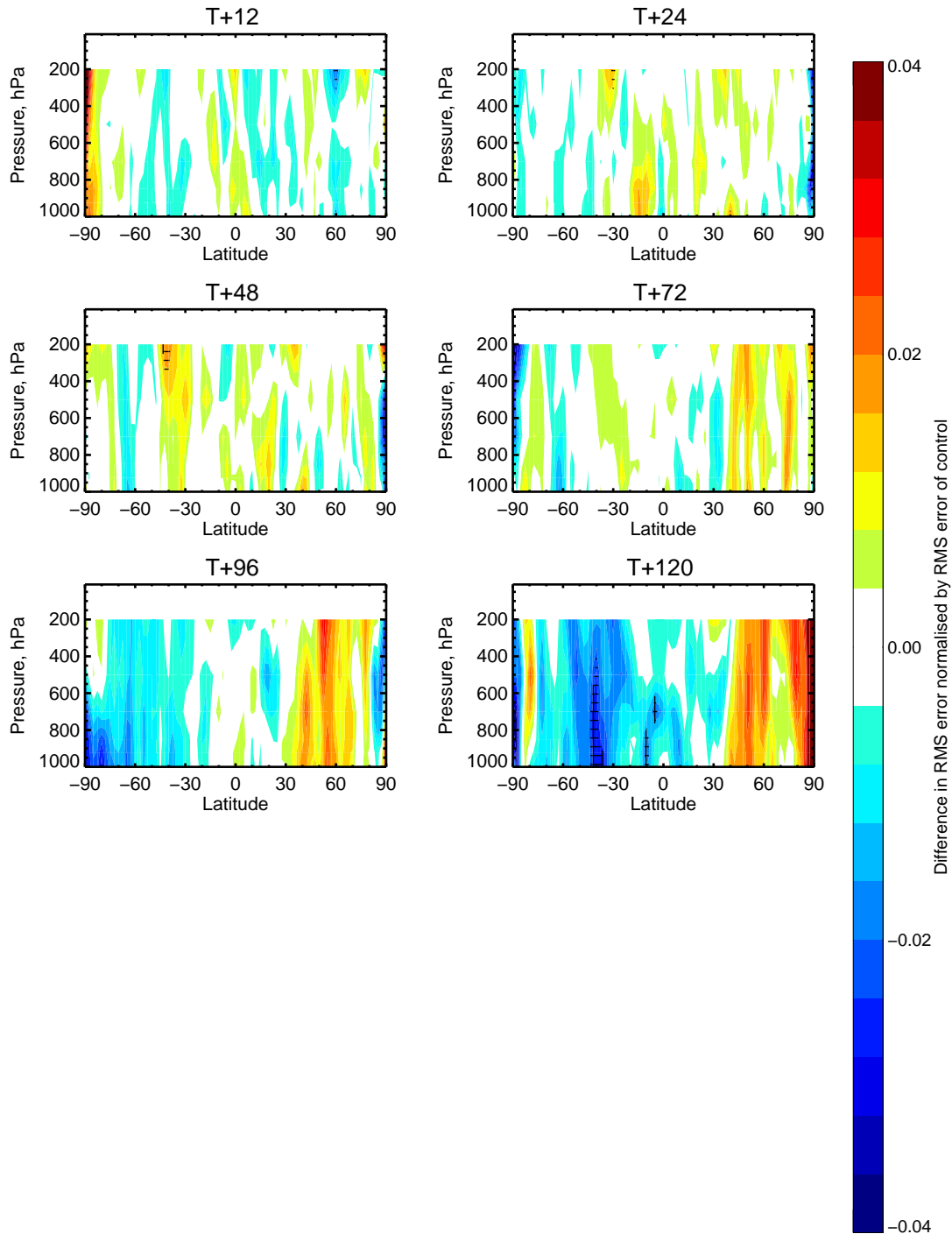


Figure 22: As Fig. 15 but for geopotential.

7 References

References

- [Albergel et al. 2012a] Albergel, C., P. de Rosnay, C. Gruhier, J. M. noz Sabater, S. Hasenauer, L. Isaksen, Y. Kerr, and W. Wagner, 2012a : Evaluation of remotely sensed and modelled soil moisture products using global ground-based in-situ observations. *Remote Sensing of Environment*, **18**,215–226. doi:10.1016/j.rse.2011.11.017.
- [Albergel et al. 2012b] Albergel, C., P. de Rosnay, C. Gruhier, J. M. noz Sabater, S. Hasenauer, L. Isaksen, Y. Kerr, and W. Wagner, 2012b : Soil moisture analyses at ECMWF: Evaluation using global ground-based in situ observations. *J. Hydrometeor.*, **13**,1442–1460. doi:10.1175/JHM-D-11-0107.1.
- [Balsamo et al. 2009] Balsamo, G., P. Viterbo, A. Beljaars, B. van den Hurk, M. Hirschi, A. Betts, and K. Scipal, 2009 : A revised hydrology for the ECMWF model: Verification from field site to terrestrial water storage and impact in the integrated forecast system. *Journal of Hydrometeorology*, **10**,623–643. doi: 10.1175/2008JHM1068.1.
- [Boussetta et al. 2013] Boussetta, S., G. Balsamo, A. Beljaars, and J. Jarlan, 2013 : Impact of a satellite-derived leaf area index monthly climatology in a global numerical weather prediction model. *International Journal of Remote Sensing*.
- [de Rosnay et al. 2009a] de Rosnay, P., M. Drusch, A. Boone, G. Balsamo, B. Decharme, P. Harris, Y. Kerr, T. Pellarin, J. Polcher, and J.-P. Wigneron, 2009a : AMMA Land Surface Model Intercomparison Experiment coupled to the Community Microwave Emission Model: ALMIP-MEM. *J. Geophys. Res.*, **114**. D05108, doi:10.1029/2008JD010724.
- [de Rosnay et al. 2009b] de Rosnay, P., M. Drusch, and J. Muñoz-Sabater, 2009b : Milestone 1 Technical Note Part I: SMOS global surface emission model. Technical report, European Centre for Medium-Range Weather Forecast, Reading, United Kingdom.
- [de Rosnay et al. 2013] de Rosnay, P., M. Drusch, D. Vasiljevic, G. Balsamo, C. Albergel, and L. Isaksen, 2013 : A Simplified Extended Kalman Filter for the global operational soil moisture analysis at ECMWF. *Quart J. Roy. Meteor. Soc.*, **139**,1199–1213. doi: 10.1002/qj.2023.
- [de Rosnay et al. 2014] de Rosnay et al., P., 2014 : SMOS Report on bias correction. Technical report, European Centre for Medium-Range Weather Forecasts, Reading, United Kingdom. in preparation.
- [Drusch et al. 2009a] Drusch, M., P. de Rosnay, G. Balsamo, E. Andersson, P. Bougeault, and P. Viterbo, 2009a : Towards a Kalman filter based soil moisture analysis system for the operational ECMWF Integrated Forecast System. *Geophys. Res. Lett.*, **36**. doi:10.1029/2009GL037716, 2009.
- [Drusch et al. 2009b] Drusch, M., T. Holmes, P. de Rosnay, and G. Balsamo, 2009b : Comparing ERA-40 based L-band brightness temperatures with Skylab observations: A calibration / validation study using the Community Microwave Emission Model. *J. Hydrometeor.*, **10**,213–226. doi: 10.1175/2008JHM964.1.
- [Geer et al. 2010] Geer, A., P. Bauer, and P. Lopez, 2010 : Direct 4D-Var assimilation of all-sky radiances. Part II: Assessment. *Quart J. Roy. Meteor. Soc.*, **136**,1886–1905.
- [IFS documentation 2012] IFS documentation, 2012 : *IFS Documentation Cycle 38R2*. ECMWF, Shinfield Road, RG2 9AX, Reading, UK. photocopy.

- [Kerr et al. 2010] Kerr, Y., P. Waldteufel, J.-P. Wigneron, S. Delwart, F. Cabot, J. Boutin, M. Escorihuela, J. Font, N. Reul, C. Gruhier, S. Juglea, M. Drinkwater, A. Hahne, M. Martin-Neira, and S. Mecklenburg, 2010 : The SMOS mission: New tool for monitoring key elements of the Global Water Cycle. *Proc. IEEE*, **98**,666–687.
- [Muñoz-Sabater et al. 2011a] Muñoz-Sabater, J., M. Dahoui, P. de Rosnay, and L. Isaksen, 2011a : SMOS Monitoring Report; Part II. Technical report, European Centre for Medium-Range Weather Forecasts, Reading, United Kingdom.
- [Muñoz-Sabater et al. 2013a] Muñoz-Sabater, J., M. Dahoui, P. de Rosnay, and L. Isaksen, 2013a : SMOS Monitoring Report; Number III: Dec. 2011 - Dec. 2012. Technical report, European Centre for Medium-Range Weather Forecasts, Reading, United Kingdom.
- [Muñoz-Sabater et al. 2014] Muñoz-Sabater, J., M. Dahoui, P. de Rosnay, and L. Isaksen, 2014 : SMOS Monitoring Report; Number IV: Jan. 2013 - Dec. 2013. Technical report, European Centre for Medium-Range Weather Forecasts, Reading, United Kingdom.
- [Muñoz-Sabater and de Rosnay 2011] Muñoz-Sabater, J., and P. de Rosnay, 2011 : Tech note- Part III-WP1300: SMOS Report on Noise Filtering. Technical report, European Centre for Medium-Range Weather Forecasts, Reading, United Kingdom.
- [Muñoz-Sabater et al. 2011b] Muñoz-Sabater, J., P. de Rosnay, and M. Dahoui, 2011b : SMOS Continuous Monitoring Reports; Part I. Technical report, European Centre for Medium-Range Weather Forecasts, Reading, United Kingdom.
- [Muñoz-Sabater et al. 2010] Muñoz-Sabater, J., P. de Rosnay, and A. Fouilloux, 2010 : Milestone 2 Technical Note, Part I:operational pre-processing chain, Part II:collocation software development, Part III: Offline monitoring suite. Technical report, European Centre for Medium-Range Weather Forecasts, Reading, United Kingdom.
- [Muñoz-Sabater et al. 2013b] Muñoz-Sabater, J., P. de Rosnay, A. Fouilloux, M. Dahoui, L. Isaksen, C. Albergel, I. Mallas, and T. Wilhelmsson, 2013b : Phase I, Final Report. Technical report, European Centre for Medium-Range Weather Forecasts, Reading, United Kingdom.
- [Muñoz-Sabater et al. 2009] Muñoz-Sabater, J., P. de Rosnay, A. Fouilloux, M. Dragosavac, and A. Hofstadler, 2009 : Milestone 1 Technical Note 1 Part II: IFS interface. Technical report, European Centre for Medium-Range Weather Forecasts, Reading, United Kingdom.
- [Muñoz-Sabater et al. 2011c] Muñoz-Sabater, J., P. de Rosnay, and G.Balsamo, 2011c : Sensitivity of L-band NWP forward modelling to soil roughness. *Int. J. Remote Sens.*, **32**,5607–5620. iFirst 2011., doi: 10.1080/01431161.2010.507260.
- [Muñoz-Sabater et al. 2013c] Muñoz-Sabater, J., P. de Rosnay, and L. Isaksen, 2013c : SMOS report on hot-spots. Technical report, European Centre for Medium-Range Weather Forecasts, Reading, United Kingdom.
- [Muñoz-Sabater et al. 2012] Muñoz-Sabater, J., A. Fouilloux, and P. de Rosnay, 2012 : Technical implementation of SMOS data in the ECMWF Integrated Forecasting System. *Geosc. Remote Sens. Letters*, **9**,252–256.
- [Muñoz-Sabater et al. 2011d] Muñoz-Sabater, J., T. Wilhelmsson, and P. de Rosnay, 2011d : Tech note- Part II-WP1200: SMOS report on Data Thinning. Technical report, European Centre for Medium-Range Weather Forecasts, Reading, United Kingdom.
- [Pellarin et al. 2003] Pellarin, T., J.-P. Wigneron, J.-C. Calvet, and P. Waldteufel, 2003 : Global soil moisture retrieval from a synthetic l-band brightness temperature data set. *Journal of Geophysical Research*, **108**.

- [Wang and Schmugge 1980] Wang, J. R., and T. Schmugge, 1980 : An empirical model for the complex dielectric permittivity of soils as a function of water content. *IEEE Transactions on Geoscience and Remote Sensing*, **18**,288–295.
- [Wigneron et al. 2007] Wigneron, J.-P., Y. Kerr, P. Waldteufel, K. Saleh, M.-J. Escorihuela, P. Richaume, P. Ferrazzoli, P. de Rosnay, R. Gurney, J.-C. Calvet, J. Grant, M. Guglielmetti, B. Hornbuckle, C. Mtzler, T. Pellarin, and M. Schwank, 2007 : L-band microwave emission of the biosphere (L-MEB) model: Description and calibration against experimental data sets over crop fields. *Remote Sensing of Environment*, **107**,639–655.
- [Wigneron et al. 2001] Wigneron, J. P., L. Laguerre, and Y. Kerr, 2001 : A simple parameterization of the L-band microwave emission from rough agricultural soils. *IEEE Transactions on Geoscience and Remote Sensing*, **39**,1697–1707.